Electronic Thesis and Dissertation Repository

6-18-2018 3:00 PM

Process Analytics from Passive Acoustic Emissions Monitoring during Fluidized Bed Pellet Coating in Pharmaceutical Manufacturing

Allan Carter
The University of Western Ontario

Supervisor
Briens, Lauren
The University of Western Ontario

Graduate Program in Biomedical Engineering
A thesis submitted in partial fulfillment of the requirements for the degree in Master of Engineering Science
© Allan Carter 2018

Abstract

Piezoelectric microphones were attached to a top spray fluidized bed to provide valuable process signatures. Relationships were developed between sound waves and conditions within the fluidized bed to relay critical quality and performance information. Deep learning analytics were used to extract valuable information from experimental data. Advancements in passive acoustic emissions monitoring will play a key role in optimizing pharmaceutical manufacturing pathways to ensure drug quality and performance.

Co-Authorship Statement

The authors have submitted Chapters 3 and 4 to refereed journals. The contributions of each author are below:

Chapter 3: In-line Acoustic Monitoring to Determine Fluidized Bed Performance During Pharmaceutical Coating

Authors: Allan Carter, Lauren Briens

Status: Submitted for publication in the International Journal of Pharmaceutics
Allan Carter performed all experimental work including data analysis. Lauren Briens provided consultation regarding experimental work and interpretation of experimental data. The manuscript was written and revised by Allan Carter and reviewed by Lauren Briens.

Chapter 4: An Application of Deep Learning to Detect Process Upset during Pharmaceutical Manufacturing using Passive Acoustic Emissions

Authors: Allan Carter, Lauren Briens

Status: Submitted for publication in the International Journal of Pharmaceutics
Allan Carter performed all experimental work including data analysis. Lauren Briens provided consultation regarding experimental work and interpretation of experimental data. The manuscript was written and revised by Allan Carter and reviewed by Lauren Briens.

Acknowledgments

Table of Contents

List of Figures

List of Appendices

Chapter 1

Introduction

1.1 Research Motivation

As primary stakeholders in social health care, political administrations must adjust policy to reduce prescription drug costs (1). One strategy would be to increase generic drug production (2, 3). Generic is a term used to describe drugs that provide the same active, dosage, and performance of a brand-name counterpart. They typically enter the pharmaceutical market once the equivalent brand-name drug loses its patent. Traditional private sector drug manufacturers justify high consumer pricing based on the costly R&D process to discover and approve new chemical and biopharmaceutical entities (4). Companies that produce generics focus on large scale production rather than innovation. The generic drug formulation is already available, and US Food and Drug Administration (FDA) approval is prompt. As generics become available, drug prices decrease, and health care affordability thrives. Individuals and insurance companies can pay less for comparable treatment.

Unlike brand-name drugs, generic costs are primarily based on long-term manufacturing economics. This shift moves process efficiency and process technology to a new level of importance. Engineering advancements in process analytical technologies (PAT)s, such as passive acoustic monitoring, will play a key role in optimizing manufacturing pathways, ensuring product quality, preventing failed batches (rejects, scrap, re-processing), and increasing automation to reduce human error. Each of these factors will contribute to lower manufacturing costs..

1.2   Process Analytics

With investment historically coupled to the discovery of new blockbuster products, advancements in manufacturing efficiency lagged behind modern technological capabilities (5). Many drug manufacturing processes run in batches and have little to no automation. Batch processing is costly, slow, and leaves room for human error. The FDA regulations also require that drug manufacturers submit comprehensive manufacturing procedures as part of the drug approval process (6) which undesirably limits continuous manufacturing improvement and process evolution as seen in comparable industries.

In 2004, the FDA's Center for Drug Evaluation and Research (CDER) released a guidance article for the development of PATs. The purpose of a PAT is to monitor manufacturing conditions that will have a substantial impact on drug quality (5, 6). A successful PAT could reduce manual sampling requirements, or compliment routine sampling procedures to improve product quality validation.

The FDA describes a PAT's function as at-line, on-line, or in-line. An at-line technology requires a pause in the process, removal of sample material, and laboratory analysis. For on-line technologies, the process remains operational during sample removal. An in-line PAT can conduct measurements without sample removal, or process interruption (6).

1.3   Modified Dosage Forms

Relationships discovered through pharmacokinetics in the 1950s subsequently led to the development of a series of modified release dosage forms (7). While conventional oral

tablets are designed to release the active pharmaceutical ingredient (API) immediately, modified release dosage forms control dispersion timing or release rate to accomplish the desired therapeutic effect (8). The drug manufacturing process plays a significant role in achieving these effects (9).

Enteric release coatings are a subset of the modified release dosage forms. Drugs coated with an enteric release polymer will delay the API's dissolution until it passes through the stomach. An enteric release dosage form will protect APIs that are acid sensitive and avoid the risk of stomach irritation from formulation ingredients.

Sustained release drugs are a second class under modified released dosage forms. These are used to extend the liberation of an API over time to reduce drug administration frequency. Sustained release coatings control the rate of API diffusion. The diffusion rate (*dM/dt*) can be modeled using Fick's second law (10) as a representation of the API mass transfer:

$$\frac{dM}{dt} = \frac{DAC_o}{h} \qquad\qquad 1.1$$

The variables in this equation are mass (M), time (t), diffusion coefficient (*D*): dependent on the coating material, the surface area of the film (*A*), the initial concentration of the API (C_o), and the film coat thickness (*h*). This representation of mass transfer can introduce the importance of film coat uniformity during drug manufacturing. Based on

Fick's second law, the areas of lowest thickness result in higher mass transfer rates; thus, reduce the desired sustained-release prosperities.

1.4   Multi-Particulate Delivery

Oral multi-particulate drug delivery provides a couple of key advantages over tablet dosage forms. With multi-particulate delivery, the small pellets or granules contain the API. These pellets are administered using a soft gelatin capsule, and upon release disperse within the patient's gastrointestinal track. This dispersion allows for a more predictable gastric emptying rate and reduces the likelihood of dose dumping.

1.5   Fluidized Bed Coating

Fluidized beds are used in the pharmaceutical industry to apply functional coatings onto multi-particulate systems. In the standard top-spray fluidized bed configuration, a batch of pellets containing the API is placed within a conical vessel. A continuous inlet air stream is pressed through a distributor plate located at the base. Upward drag forces of the air stream initiate pellet movement. Coating solution is applied using an atomizing nozzle located above the pellets while drying occurs in the same chamber. Drug manufaturers favor fluidized bed operations for high mass and heat transfer efficiency. The pellet movement allows for uniform coating application, and the inlet air provides a mechanism for effective heat transfer to dry the coating solution.

The multivariate nature of simultaneous mixing, mass transfer, and drying increases process complexity. Effective fluidized bed operation can be controlled through the

manipulation of variables such as: air temperature (T_o), air velocity (v_o), bulk pellet mass

(m), spray rate ($\dot{m}_i$), spray duration (t_i), and period between spray (t_s). In practice, the

control of a fluidized bed is commonly based on operator experience rather than process

knowledge (11, 12). This reliance on user experience introduces a risk of human error.

The most critical process parameter in fluidized bed operation is minimum fluidization

velocity (u_{mf}): the lowest inlet air velocity required to overcome the downward force from

bulk pellet mass (m) within the bed. Below u_{mf}, the solid pellets are fixed; however, above

u_{mf}, the bed becomes fluidized. The accepted engineering calculation of u_{mf} comes from

Ergun's equation (13):

$$\left(\rho_s - \rho_g\right)g \;=\; \frac{\rho_g u_{mf}^2}{\phi D \varepsilon^3}\left(\frac{150(1-\varepsilon)\mu_g}{\phi D_p u_{mf}\rho_g} + 1.75\right) \tag{1.2}$$

Whereby the variables included are inlet air viscosity (μ_g), mean particle diameter (Dp),

the density of the gas (ρ_g), void fraction with the particle bed (ε_{mf}), particle sphericity (ϕ),

particle density (ρ_s), and acceleration of gravity (g).

1.6   Acoustic Emissions

Interactions inside the chamber during fluidized bed operation generate complex sound

waves. The passive acoustic emissions will arise from three independent sources. Impact

sound originates from particle-particle and particle-chamber collisions within the bed.

Friction sound originates from particle-particle contact as particles pass one another, and

particle-chamber contact as pellets move adjacent to the fluidized bed walls.

Aerodynamic noise arises from turbulence as inlet air passes through the particle bed and freeboard (14). Sound waves generated by each of these sources disperse through the equipment boundaries. A microphone recording below 40 kHz can detect real-time process changes from within the bed (15, 16). Passive acoustic emissions amplitude and frequency will shift in time; thus, providing quantitative variations to extract physical meaning. Piezoelectric microphones function by converting acoustic pressure waves into electric current. Signals must be amplified and relayed to a data logger before analysis in the time domain or frequency domain.

1.7   Thesis Overview

The previous work using acoustic monitoring successfully demonstrated feasibility under a narrow scope (15, 16). Further work is required to understand how acoustic monitoring will be affected under various process conditions. Fluidized bed unit optimization is challenging due to the multivariate nature of the fluidized system. This study investigates acoustic signals received from pellet coating under variable operating conditions and process failure conditions. The experimental data relates acoustic monitoring with interactions inside the fluidized bed chamber to form engineering relationships.

Chapter 2 provides a literature review to introduce aspects of fluidized bed coating and the process monitoring methods under evaluation by several research groups. This chapter also provides an introduction into the pharmaceutical industry's manufacturing challenges and data analytical methods. This chapter introduces theory and compares work with other authors.

Chapter 3 is the first experimental section of this thesis. The work explores the application of passive acoustic emissions monitoring as a method to improve temperature management during pellet coating. Fluidized beds are often energy-inefficient. An improved passive acoustic emissions monitoring and control strategy would support manufacturing cost efficiencies and reduce energy waste.

Chapter 4 provides the second experimental section. This work explores the application of passive acoustic emissions as a method to provide early process failure detection. In this section, acoustic emissions are analyzed using a deep learning program to classify conditions inside the process boundary. The artificial neural network was used to extract meaning from a highly complex passive acoustic signal.

Chapter 5 provides conclusions for the findings presented in this research. Passive acoustic emission monitoring can provide a wealth of control data for pharmaceutical manufacturers to optimize and improve operations. Advances in deep learning and artificial intelligence for multivariate data analytics help simplify the complex task of extracting meaning from passive acoustic data.

1.9   References

1. Obama B. United States Health Care Reform. JAMA. 2016;316(5):525.

2. Ferrándiz J. The impact of generic goods in the pharmaceutical industry. Health Economics. 1999;8(7):599-612.

3. Davit B, Nwakama P, Buehler G, Conner D, Haidar S, Patel D et al. Comparing Generic and Innovator Drugs: A Review of 12 Years of Bioequivalence Data from the United States Food and Drug Administration. Annals of Pharmacotherapy. 2009;43(10):1583-1597.

4. DiMasi J, Hansen R, Grabowski H. The price of innovation: new estimates of drug development costs. Journal of Health Economics. 2003;22(2):151-185.

5. Hinz D. Process analytical technologies in the pharmaceutical industry: the FDA's PAT initiative. Analytical and Bioanalytical Chemistry. 2005;384(5):1036-1042.

6. U.S. Department of Health and Human Services Food and Drug Administration. Guidance for Industry PAT — A Framework for Innovative Pharmaceutical Development, Manufacturing, and Quality Assurance. 2004

7. Wagner J. History of pharmacokinetics. Pharmacology & Therapeutics. 1981;12(3):537-562.

8. Shargel L, Yu A. Applied biopharmaceutics & pharmacokinetics. Stamford, Conn.: Appleton & Lange; 1999.

9. Yu L, Amidon G, Khan M, Hoag S, Polli J, Raju G et al. Understanding Pharmaceutical Quality by Design. The AAPS Journal. 2014;16(4):771-783.

10. Carstensen J. Advanced pharmaceutical solids. New York: Marcel Dekker; 2001.

11. Räsänen E, Rantanen J, Mannermaa J, Yliruusi J. The Characterization of Fluidization Behavior Using a Novel Multichamber Microscale Fluid Bed. Journal of Pharmaceutical Sciences. 2004;93(3):780-791.

12. Larsen C, Sonnergaard J, Bertelsen P, Holm P. A new process control strategy for aqueous film coating of pellets in fluidised bed. European Journal of Pharmaceutical Sciences. 2003;20(3):273-283.

13. Ergun S, Orning A. Fluid Flow through Randomly Packed Columns and Fluidized Beds. Industrial & Engineering Chemistry. 1949;41(6):1179-1184.

14. Tsujimoto H, Yokoyama T, Huang C, Sekiguchi I. Monitoring particle fluidization in a fluidized bed granulator with an acoustic emission sensor. Powder Technology. 2000;113(1-2):88-96.

15. Sheahan T, Briens L. Passive acoustic emissions monitoring of the coating of pellets in a fluidized bed—A feasibility analysis. Powder Technology. 2015;283:373-379.

16. Sheahan T, Briens L. Passive acoustic emission monitoring of pellet coat thickness in a fluidized bed. Powder Technology. 2015;286:172-180.

Chapter 2

Literature Review

2.1　　Fluidized Bed Coating

2.1.1　Process Overview

Fluidization is a method of suspending solid particles within a moving gas, liquid, or combination of gas and liquid. Upward forces from the mobile phase cause the particles to enter a dynamic state. In the pharmaceutical industry, fluidization can be used to support the application of spray coatings. Constant particle mixing from a fluidized bed enhances spray coating distribution. (1). Fluidized beds used in pellet coating applications are typically designed with bottom spray and top spray configurations.

The bottom spray fluidized beds often use a Wurster column insert (Figure 2.1). The Wurster column forces pellets upwards through a central flow pattern while an adjacent nozzle applies a coating to pellets passing through the insert. The Wurster configuration provides excellent film coating uniformity but increases the risk of attrition from the high collision forces as the pellets move upwards through chamber (2 – 4). Attrition will result in dose variability between pellets. Significant attrition will result in failed quality assurance.

Top spray fluidized beds use an atomizing spray nozzle located within the freeboard. The coating solution is sprayed onto the bed of pellets from above. The surface region accepting the coating is called the fluidized bed interface. Particles are continuously

recycled at the interface region. The fluidization air moves uncoated particles from the

bottom of the chamber to the surface, while coated particles drop back into the chamber.

Continuous mixing within the chamber ensures a uniform coating on all particles.
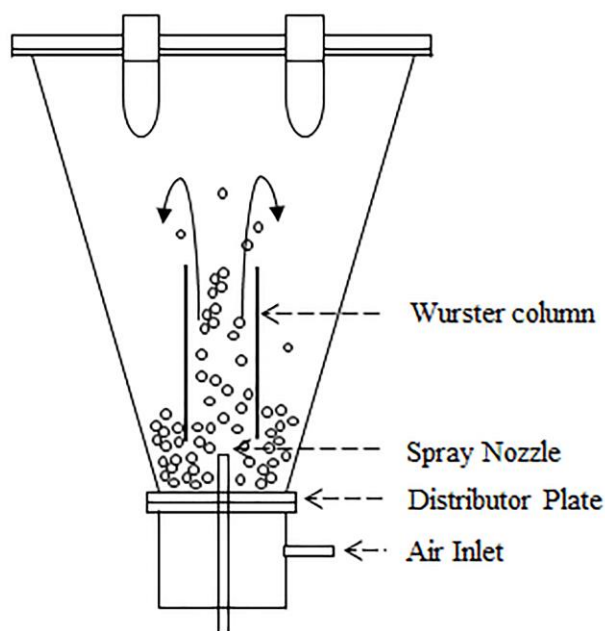
Figure 2.1 Schematic of a fluidized bed with Wurster column and bottom spray configuration

In 1973, Geldart wrote about the dynamic behavior of fluidized bed systems based on

particle size and density characteristics (5). Visible behaviors were related to size-

dependent interparticle forces. Today, solid-gas fluidized beds are still described using

the Geldart classification system. The smallest, 20 to 30 µm Geldart C particles, can be

challenging to fluidize and are likely to exhibit channeling. The largest, >600 µm Geldart

D particles, will display a bubbling action; air pockets rise through the bed and gently

spout particles into the chamber above upon reaching the bed's surface. Pellets used in pharmaceutical applications usually fall under the Geldart D classification.

Process control is highly multivariate, and few monitoring tools exist to help operators make batch adjustments while the coating is in progress. Precise control of operating conditions ensures consistent product quality. Temperature can be adjusted to improve drying rate of the coating solution; however, excessively high temperatures can be un-economical from an energy standpoint. In some formulations, excessive temperatures may also cause drug degradation, inactivation, or damage the coating. Fluidization velocity can be increased to break apart agglomerates; however, excessive velocity will result in attrition (6). Improvements in PATs will help operators monitor changes inside the equipment and provide data to make better real-time decisions. Fluidized beds are often more economical than other coating processes, as coating and drying occurs within the same chamber. This removes the need for additional downstream drying equipment.

In pharmaceutical manufacturing, APIs can be coated onto the surface of non-pareils pellets such as Suglets® or Cellets®. The pellets are used as a structural surface. Once coated with API, the pellets are filled into small gelatin capsules for treatment as a multiple unit dosage. The small size and high quantity of the API pellets allows for improved gastrointestinal distribution upon ingestion. Drug absorption will improve through higher surface contact from multiple pellets. The pellets dispersion will also reduce this risk of localized drug leaching should the capsule become physically lodged at any set location (7, 8). Pellet coatings provide pharmacokinetic functionalities, such as delayed or modified release.

2.1.2   Forces During Coating

During the spray period, atomized liquid droplets cover the surface of pellets at the interface. Particle movement then promotes the spread of coating solution across all particles in the bed. Van der Waals, electrostatic, and liquid bridge forces each play a role in particle-particle interactions; however, liquid bridge forces have the greatest impact (9, 10). When pellets covered in a liquid film collide, the film at the contact point combines to create a liquid bridge. The surface tension caused by the liquid between the two pellets provides a bridging force that will hold the pellets together. Agglomeration may occur when liquid bridges between small groups of particles dry and solidify. As shown in Figure 2.2, agglomerates will reduce film coat uniformity, thus effecting drug release rate (11 – 13). High agglomerate formation will also increase the minimum gas velocity required to sustain fluidization.
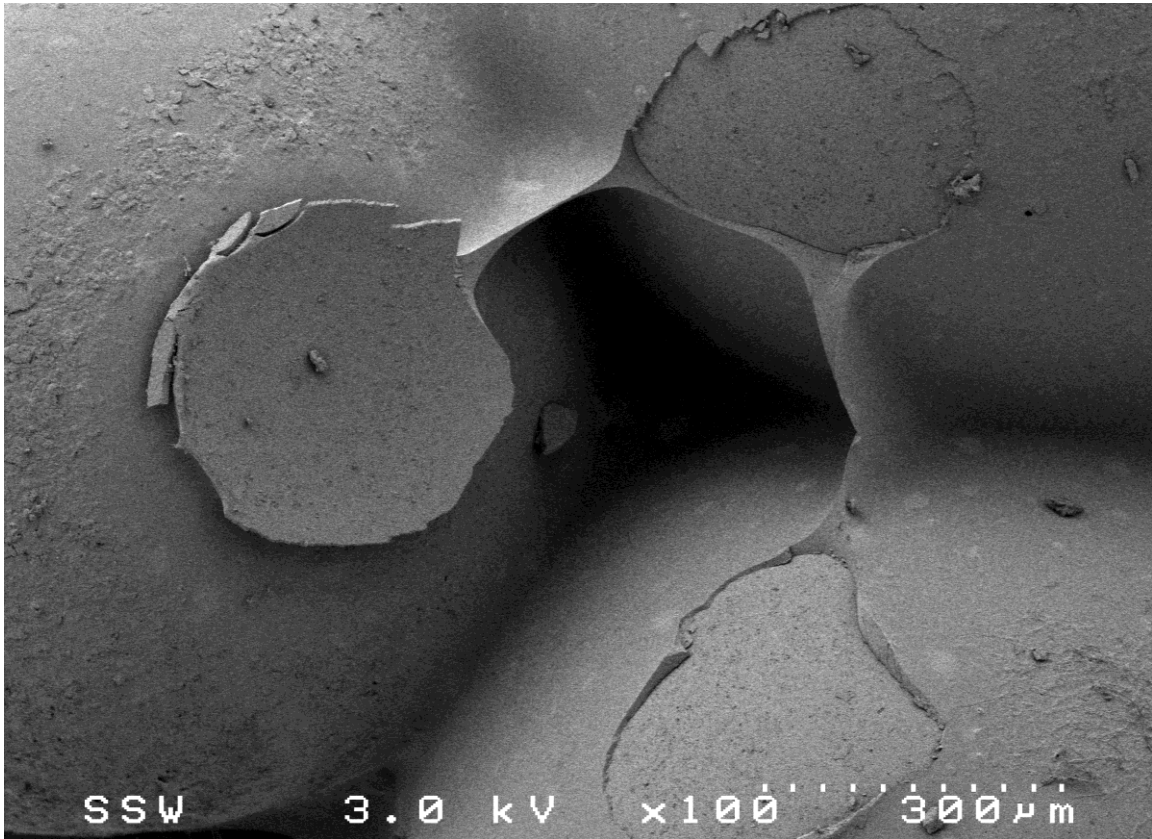
Figure 2.2 Non-uniform application of Acryl-EZE coating on 1000 μm glass spheres as the result of particle agglomeration

Drying in a fluidized bed occurs as the surface liquid is removed from the solid particles through evaporation. The rate for liquid removal is dependent on system temperature, and adjacent vapor concentration. Neglecting kinetic energy, the surface liquid must be heated beyond a temperature where vapor pressure exceeds the partial pressure of surrounding gas. In a fluidized bed, the surrounding gas is continually being removed and replaced in the system. This convective heat transfer decreases the adjacent vapor concentration; thus, allowing the drying rate to increase. It can be viewed as the change in moisture content (W) versus time (t):

$$Drying \ = \ \frac{dW}{dt} \tag{2.1}$$

Solid drying is based on two simultaneous mechanisms. The first is heat transfer, which initiates liquid evaporation on the surface of the solid. The second mechanism is mass transfer, which allows liquid from within the solid to move towards the surface. A linear drying stage occurs when the surface of the solid is saturated with liquid. During this stage, the drying rate is solely dependent on heat transfer from the surrounding gas to the evaporating surface liquid.

$$\frac{dW}{dt} = \frac{h_t A \Delta T}{\lambda} \ \ or \ \ k_g A \Delta p \tag{2.2}$$

where the equation variables are total heat transfer coefficient (h_t), area for heat transfer (A), latent heat of evaporation at reference temperature (λ), difference between system temperature and reference temperature (ΔT), mass transfer coefficient (k_g), and difference between vapor pressure of evaporating liquid and partial pressure of liquid in the surrounding gas (Δp) (19).

As drying progresses, the liquid on the surface of the solid decreases. This begins the second non-linear stage, where liquid moves from the solids center to the surface for removal. During this stage, drying rate is a function of diffusion. As liquid within the solid decreases so does the diffusion rate. This drying relationship can consequently be modeled using Fick's second law (14).

$$\frac{dW}{dt} = f\left(\frac{dc}{dt}\right) = f\left(\frac{Dd^2C}{dx}\right) \tag{2.3}$$

where the equation variables are the concentration at the liquid-gas interface (c), diffusion coefficient (D), concentration in the solid (C) at distance x, and the distance into the solid in the direction of diffusion (x) (14).

In non-porous solids, the liquid remains on the surface as a film. Only the first linear drying stage would apply. In pharmaceutical manufacturing, non-porous pellets or porous granules may be used in the fluidized bed coating process; thus, the drying profile would be dependent on the batch in production.

2.1.3   Coating Thickness

The performance of a modified release coating is dependent on variability in coating thickness and uniformity (15 – 17). In 2001 and 2002, Chen and Lee studied the release of pharmaceuticals from non-uniform coatings. Their research demonstrated that the coating uniformity has a more significant impact to drug release than average coating thickness. The thinnest coated area is the primary factor affecting API release rate (15, 16).

There has been limited development of real-time monitoring methods to determine coating thickness within a fluidized bed. The evaluation of coating thickness usually involves timely and invasive sampling. Samples will be evaluated based on mass gain, dissolution or near infrared (NIR) spectroscopy to determine the coat quality.

2.1.4   Process Stages

During the coating process, the solvent-solute mixture is atomized by the spray nozzle. The droplets fall towards the fluidized bed of pellets. Upon contact, the droplets spread across the surface of the pellets to form a film layer.

During the drying stage, the coating solvent evaporates. The solute remains on the surface of the pellets. Fluidized beds allow coating and drying operations to occur within the same piece of equipment. Solvent evaporation occurs as the inlet air rushes past the fluidized particles. Moisture is released from the surface, captured by the continuous air stream, and removed from the system through a filtered exhaust. The thermodynamics model of coating and drying has been described by various authors (18 – 22). An early publication by Ebey described the coating process under steady-state conditions based on first law principles (18). These models can be useful for simple troubleshooting purposes; however, engineering models lack the accuracy that could be provided by PAT instrumentation. Fluidized bed process control strategies for drug coating applications are heavily based on operator experience (22 – 24).

2.2   Process Monitoring

The following section is a review of various monitoring approaches used by the pharmaceutical industry or under study through the research. The section briefly discusses at-line sampling, but primarily focuses on in-line technologies that are capable of real-time monitoring. Each method provides a unique approach to capture data. Their benefits, and limitations are listed.

2.2.1   Periodic Sampling

Fluidized bed operation is primarily monitored through the removal of at-line samples. This activity is time consuming and can be disruptive to the process. The samples removed from the bed are used for a range of laboratory testing to assess quality. Dissolution testing and NIR spectroscopy from samples are both effective in evaluating film coating development (25 – 28). However, both quality evaluation methods require too much analysis time for real time process control applications.

2.2.2   Differential Pressure

Pressure monitoring has been used as a technique to monitor fluidized bed drying performance and changes in pellet flow patterns. The differential pressure across the bed is equal to the weight of the bed when the inlet air reaches the minimal fluidization velocity (23, 29).   A change in differential pressure from below and above the particle bed can be used to indicate a shift in fluidization performance. Increases in air flow beyond the minimal fluidization velocity will not provide a noteworthy change in differential pressure. Shifts below the minimal fluidization velocity will provide a sharp increase in the recorded pressure drop. Briens and Ellis reviewed fluidized bed hydrodynamics by monitoring differential pressure while applying chaos analysis and wavelet signal processing methods to classify different systems (30).

Researchers have also studied pressure fluctuation analysis as a method to detect changes in the process, such as agglomeration or end-point determination (31 – 34). These changes are abrupt and can be difficult to distinguish from the bubbling action prominent

in Geldart D fluidized beds. Fluidized bed pressure monitoring has also been used to determine dominant bubble frequencies and relate these frequencies to distributor performance (35). Pressure monitoring is straightforward and economical; however, it requires the placement of a pressure sensor inside the process boundary. The probe can become fouled from the coating solution and will require cleaning between each batch.

2.2.3   Temperature and Humidity

Exhaust air temperature and humidity monitoring can be used as a method to evaluate fluidized bed drying. Drying progress can be inferred based on changes in these variables. A temperature increase and humidity decrease can be used to indicate the bed drying rate. Coating passively cools the air stream as the air passes across the pellets and flows into the exhaust. The extent that the air is cooled gradually reduces as solvent is removed through evaporation. The monitoring method can be used to estimate the end-point of the drying process (36).

2.2.4   Near Infrared Spectroscopy

Near infrared (NIR) spectroscopy has gained widespread attention as a non-destructive in-line method to monitor pellet coating performance. NIR spectroscopy applies light from 780-2500 nm to probe deep into a sample. A spectrum is recorded using a detector placed adjacent to the light source, and individual features within the spectra are linked to target chemical compounds (37). NIR light is non-destructive and does not react with any contents within the fluidized bed. The monitoring setup requires a continuous NIR detector attached to a transparent viewing window. Changes in the recorded spectra are

related to coating thickness (38 – 41). Beyond monitoring coating progress, NIR has also been employed to track changes in process moisture for fluidized bed granule drying applications (42, 43). One issue while using this method is progressive fouling of the detector's window. Buildup of coating solution or residual particulate from the granules can block off the detector and significantly reduce monitoring performance. As another drawback, the sampling material and measurement environment will affect the NIR spectra. Situational calibration is required, which adds complexity while extracting process features from the data (38).

2.2.5   Raman Spectroscopy

Raman spectroscopy is similar and can be viewed as complementary, to NIR spectroscopy. While NIR analysis is based on light absorbance, Raman spectroscopy is based on Raman scattering. Changes in molecular vibration are recorded by a detector as light enters into the system. The vibrational changes are then related to the composition of the sample. Promising research has demonstrated the application of Raman spectroscopy in determination of pellet coating thickness while operating a fluidized bed (44 – 46). However, the same limitations as NIR spectroscopy apply: the detector requires a transparent window into the process, and this window can become fouled and significantly reduce production monitoring performance.

2.2.6   Acoustic Emissions

Passive acoustic emissions have been investigated as a non-destructive and non-invasive monitoring technology for pharmaceutical manufacturing. For fluidized bed coating,

acoustic emissions arise from particle-particle collisions, particle-vessel collisions, and air flow through the fluidized bed and freeboard (47). Microphones placed outside the process boundary can passively detect changes in these acoustics (47 – 51). The current challenge is to relate the changes in the acoustic emissions with real-time process conditions that will have an impact on product quality.

Naelapää et al. established the use of passive acoustic emissions as a monitoring tool for fluidized bed coating processes. In their work, potassium chloride crystals were coated using ethylcellulose and monitored at a frequency of 16.5 kHz and 50kHz (48). The work also helped demonstrate that the higher frequency monitoring outperformed lower frequency trials. Tsujimoto et al. studied passive acoustic control for fluidized bed applications using very high-frequency elastic waves between 100 kHz - 140 kHz recorded with a piezoelectric microphone (47). Frequencies within this range can provide highly localized monitoring data. As a downside, the excessive data generated from high frequency recording increased computer processing time requirements which reduced applicability in real-time process control. As computers continue to improve, data management will become less of a challenge. Daniher et al. evaluated acoustic emissions from the exhaust of a granulation process. The research demonstrated that passive acoustics from the process exhaust can also provide valuable information regarding conditions inside equipment (52). Hansuld et al. further showed that passive acoustic emissions from the air exhaust of high-shear granulation processes can be used in end-point determination; their studies compared different granule densities and related defined endpoints with acoustic emission profiles (52, 53).

Sheahan and Briens demonstrated that acoustic monitoring at 40 kHz can be an effective way to monitor the fluidized bed coating of glass pellets and a sugar-based coating solution (49, 50). Microphones that were placed externally to the fluidized bed were able to detect transitions between coating and drying stages of operation effectively. Data analyses took place within time-domain windows of reasonable length for process control applications. As a limitation, this research worked with a single set of operating conditions. Additional work was required to understand how changes in process variables will influence the acoustic signals.

2.3   Manufacturing Challenges

2.3.1   Process Optimization

Drug products are highly regulated and must meet strict quality specifications. Quality standards are governed by agencies such as the U.S. FDA, Health Canada, or directed through Good Manufacturing Practices (GMP) quality systems. Unfortunately, the processes used during manufacturing are not always optimized regarding time, energy, and cost efficiency. The majority of drug production is still completed using time-consuming batch manufacturing techniques. In parallel industries, such as food or petrochemical processing, much of the product line has transitioned to continuous and automated manufacturing. For the pharmaceutical industry to move in the same direction, greater control over processes are needed. Improved real-time PATs to monitor physical and chemical changes along the production line will give manufacturers more control. Improved control will support the development of automation and lower drug manufacturing costs.

Pharmaceutical Quality by Design (QbD) is a well-established approach to developing an effective drug product (55, 56). The plan emphasizes process control and understanding every aspect of the drug production to minimize risk and ensure consumer safety. Improved PATs fit into the framework of QbD by supporting production sites to monitor critical process parameters that are identified by the QbD framework. These process parameters have a significant impact on the drug quality; for a fluidized bed coating operation, inlet air and product temperatures are examples. At low temperatures, the fluidized bed may dry slowly and become unstable as excessive coating layers are added. Material agglomeration will occur resulting in non-uniform film layers. In contrast, high temperatures will enhance drying, but excessively high temperatures may be detrimental to the coating polymer, and over extended manufacturing cycles will be energy wasteful. A balance is required. Continued optimization using new PATs would improve the manufacturing cycle. The lowest and most energy efficient temperature without the formation of agglomerates would be ideal.

2.3.2   Process Failure

Enhanced PATs will also be used to prevent process failures. It is not uncommon to completely disregard a batch of the finished product as result of failed quality testing. An example of a process failure during fluidized bed coating is distributor plate blockage. The distributor plate is a perforated plate or mesh located at the base of the fluidized bed chamber. Its purpose is to evenly distribute air across the bed to prevent localized fluidization or the development of unstable fluidization regimes. Past studies have reviewed distributor plate design and performance by analyzing bubble size and radial

gas distribution (35, 57, 58). A distributor plate blockage could occur if the coating solution blinds the distributor plate or if excessive agglomerated pellets settle across the plate.

2.4   Data Analytics

2.4.1   Standard Deviation

One of the leading reasons why acoustic emissions monitoring is rarely used in manufacturing today arises from data analytics. Sound waves recorded from industrial processes are very complicated, and it can be immensely challenging to relate features within recorded acoustic signals to production conditions inside the targeted operation. Previous studies have shown success while using a moving standard deviation filter to analyze acoustic data for process control (50). A moving standard deviation can mathematically and visually emphasize changes in signal amplitude and frequency while remaining in the time domain. Standard deviation measures signal fluctuation away from the mean. A moving standard deviation will incorporate leading and lagging points within a fixed window to calculate a value representing fluctuation for each data segment. Changes in the moving standard deviation over time can subsequently relate back to dynamic physical or chemical parameters within the process.

2.4.2   Multivariate Analysis

Features within a sound wave can be analyzed simultaneously through a multivariate approach. Traditional multivariate methods include principle component analysis (PCA)

and partial least squares (PLS) regression. PCA is a statistical method whereby a multidimensional data set is transformed into a lower dimensionality space (59). PCA evaluates the variance between values to detect dominant patterns. The data can be visualized in a two-dimensional plot to select the highest influence principal components. For industrial applications, PCA can assist in process upset diagnosis. PLS regression is similar to PCA. Rather than plotting data into two-dimensional space, PLS uses two independent variable spaces and fits data in one space against the other (60). Relationships can be created between each variable space to help understand operating conditions in the manufacturing environment (53, 54, 60).

An emerging method for multivariate data analysis is deep learning. Deep learning is a program architecture whereby an input layer of independent data is related to an output layer of data using cost function analysis and backpropagation (62, 63). Like PLS, the objective is to create relationships between multivariate inputs and one-or-more output variables. In deep learning, the input variables are normalized and then passed into a hidden layer of nodes. Each node can be activated based on the weight of the previous layer. The activation is typically initiated using either a linear rectifier function or a probabilistic sigmoid function. Activation determines if the input passes into the subsequent layers. If it fails to pass forward, the node has little or no relationship with the output. Once the output layer has been reached, a cost function is used to calculate the difference between the calculated output value and the real output value for the given dataset. The deep learning program then cycles back and adjusts the weights between each node to lower the cost function at the end of each cycle. Through this iterative backpropagation, the program teaches itself relationships between the input variables and

output layer. By using multiple layers of interconnected nodes, the deep learning program not only evaluates the relationship between input and output, but also assesses interdependent relationships between input variables and how interdependent relationships link to the output variable. A multiple layer approach contributes to deep learning's ability to outperform traditional methods of multivariate data analysis, and other machine learning architectures (64).

2.5   References

1. Kunii D, Levenspiel O. Fluidization engineering. Amsterdam: Elsevier; 2012.

2. Christensen F, Bertelsen P. Qualitative Description of the Wurster-Based Fluid-Bed Coating Process. Drug Development and Industrial Pharmacy. 1997;23(5):451-463.

3. Hampel N, Bück A, Peglow M, Tsotsas E. Continuous pellet coating in a Wurster fluidized bed process. Chemical Engineering Science. 2013;86:87-98.

4. Albanez R, Nitz M, Taranto O. Enteric coating process of diclofenac sodium pellets in a fluid bed coater with a Wurster insert: Influence of process variables on coating performance and release profile. Advanced Powder Technology. 2013;24(3):659-666.

5. Geldart D. Types of gas fluidization. Powder Technology. 1973;7(5):285-292.

6. Turton R, Cheng X. The scale-up of spray coating processes for granular solids and tablets. Powder Technology. 2005;150(2):78-85.

7. Sirisha K, A review of Pellets and pelletization process - A multiparticulate drug delivery system. International journal of pharmaceutical sciences and research. 2013;4(6).

8. Aulton M. Pharmaceutics: The Science of Dosage Form. Edinburgh: Churchill Livingstone; 2002.

9. Hemati M, Cherif R, Saleh K, Pont V. Fluidized bed coating and granulation: influence of process-related variables and physicochemical properties on the growth kinetics. Powder Technology. 2003;130(1-3):18-34.

10. Wormsbecker M. Study of hydrodynamic behavior in a conical fluidized bed dryer using pressure fluctuation analysis and X-ray densitometry [Ph.D]. University of Saskatchewan. 2008.

11. Porter S, Felton L. Techniques to assess film coatings and evaluate film-coated products. Drug Development and Industrial Pharmacy. 2010;36(2):128-142.

12. Haddish-Berhane N, Jeong S, Haghighi K, Park K. Modeling film-coat non-uniformity in polymer coated pellets: A stochastic approach. International Journal of Pharmaceutics. 2006;323(1-2):64-71.

13. de Souza L, Nitz M, Taranto O. Film Coating of Nifedipine Extended Release Pellets in a Fluid Bed Coater with a Wurster Insert. BioMed Research International. 2014;2014:1-11.

14. Perry R, Green D. Perry's Chemical Engineers Handbook. New York: McGraw-Hill; 2008.

15. Chen B, Lee D. Slow Release of Drug through Deformed Coating Film: Effects of Morphology and Drug Diffusivity in the Coating Film. Journal of Pharmaceutical Sciences. 2001;90(10):1478-1496.

16. Chen B, Lee D. Finite element analysis of slow drug release through deformed coating film: effects of morphology and average thickness of coating film. International Journal of Pharmaceutics. 2002;234(1-2):25-42.

17. Rhodes C, Porter S. Coatings for Controlled-Release Drug Delivery Systems. Drug Development and Industrial Pharmacy. 1998;24(12):1139-1154.

18. Ebey, G. A thermodynamic model for aqueous film-coating. Pharmaceutical Technology. 1987;11(4):40-50

19. Maronga, S. On the Optimization of the Fluidized Bed Particulate Coating Process. Royal Institute of Technology Stockholm. 1998.

20. Reiland T, Seitz J, Yeager J. Aqueous Film-Coating Vaporization Efficiency. Drug Development and Industrial Pharmacy. 1983;9(6):945-958.

21. Kage H, Takahashi T, Yoshida T, Ogura H, Matsuno Y. Coating efficiency of seed particles in a fluidized bed by atomization of a powder suspension. Powder Technology. 1996;86(3):243-250.

22. Larsen C, Sonnergaard J, Bertelsen P, Holm P. A new process control strategy for aqueous film coating of pellets in fluidised bed. European Journal of Pharmaceutical Sciences. 2003;20(3):273-283.

23. Räsänen E, Rantanen J, Mannermaa J, Yliruusi J. The Characterization of Fluidization Behavior Using a Novel Multichamber Microscale Fluid Bed. Journal of Pharmaceutical Sciences. 2004;93(3):780-791.

24. Naelapää K, Veski P, Pedersen J, Anov D, Jørgensen P, Kristensen H et al. Acoustic monitoring of a fluidized bed coating process. International Journal of Pharmaceutics. 2007;332(1-2):90-97.

25. Kirsch J, Drennen J. Determination of film-coated tablet parameters by near-infrared spectroscopy. Journal of Pharmaceutical and Biomedical Analysis. 1995;13(10):1273-1281.

26. Plugge W, van der Vliest C. The use of near infrared spectroscopy in the quality control laboratory of the pharmaceutical industry. Journal of Pharmaceutical and Biomedical Analysis. 1992;10(10-12):797-803.

27. Swarbrick B. The Current State of near Infrared Spectroscopy Application in the Pharmaceutical Industry. Journal of Near Infrared Spectroscopy. 2014;22(3):153-156.

28. Jamrógiewicz M. Application of the near-infrared spectroscopy in the pharmaceutical technology. Journal of Pharmaceutical and Biomedical Analysis. 2012;66:1-10.

29. Ergun S, Orning A. Fluid Flow through Randomly Packed Columns and Fluidized Beds. Industrial & Engineering Chemistry. 1949;41(6):1179-1184.

30. Briens L, Ellis N. Hydrodynamics of three-phase fluidized bed systems examined by statistical, fractal, chaos and wavelet analysis methods. Chemical Engineering Science. 2005;60(22):6094-6106.

31. Silva C, Parise M, Silva F, Taranto O. Control of fluidized bed coating particles using Gaussian spectral pressure distribution. Powder Technology. 2011;212(3):445-458.

32. Vervloet D, Nijenhuis J, van Ommen J. Monitoring a lab-scale fluidized bed dryer: A comparison between pressure transducers, passive acoustic emissions and vibration measurements. Powder Technology. 2010;197(1-2):36-48.

33. Chaplin G, Pugsley T, Winters C. Monitoring the fluidized bed granulation process based on S-statistic analysis of a pressure time series. AAPS PharmSciTech. 2005;6(2):E198-E201.

34. Savari C, Sotudeh-Gharebagh R, Zarghami R, Mostoufi N. Non-intrusive characterization of particle size changes in fluidized beds using recurrence plots. AIChE Journal. 2016;62(10):3547-3561.

35. Wormsbecker M, Pugsley T. Distributor Induced Hydrodynamics in a Conical Fluidized Bed Dryer. Drying Technology. 2009;27(6):797-804.

36. Alden M, Torkington P, Strutt A. Control and instrumentation of a fluidized-bed drier using the temperature-difference technique I. Development of a working model. Powder Technology. 1988;54(1):15-25.

37. Workman J, Weyer L. Practical guide to interpretive near-infrared spectroscopy. Boca Raton: CRC Press; 2008.

38. Luypaert J, Massart D, Vander Heyden Y. Near-infrared spectroscopy applications in pharmaceutical analysis. Talanta. 2007;72(3):865-883.

39. Lee M, Seo D, Lee H, Wang I, Kim W, Jeong M et al. In line NIR quantification of film thickness on pharmaceutical pellets during a fluid bed coating process. International Journal of Pharmaceutics. 2011;403(1-2):66-72.

40. Naidu V, Deshpande R, Syed M, Deoghare P, Singh D, Wakte P. PAT-Based Control of Fluid Bed Coating Process Using NIR Spectroscopy to Monitor the Cellulose Coating on Pharmaceutical Pellets. AAPS PharmSciTech. 2016;18(6):2045-2054.

41. Andersson M, Folestad S, Gottfries J, Johansson M, Josefson M, Wahlund K. Quantitative Analysis of Film Coating in a Fluidized Bed Process by In-Line NIR Spectrometry and Multivariate Batch Calibration. Analytical Chemistry. 2000;72(9):2099-2108.

42. Frake P, Greenhalgh D, Grierson S, Hempenstall J, Rudd D. Process control and end-point determination of a fluid bed granulation by application of near infra-red spectroscopy. International Journal of Pharmaceutics. 1997;151(1):75-80.

43. Green R, Thurau G, Pixley N, Mateos A, Reed R, Higgins J. In-Line Monitoring of Moisture Content in Fluid Bed Dryers Using Near-IR Spectroscopy with Consideration of Sampling Effects on Method Accuracy. Analytical Chemistry. 2005;77(14):4515-4522.

44. Hisazumi J, Kleinebudde P. In-line monitoring of multi-layered film-coating on pellets using Raman spectroscopy by MCR and PLS analyses. European Journal of Pharmaceutics and Biopharmaceutics. 2017;114:194-201.

45. De Beer T, Burggraeve A, Fonteyne M, Saerens L, Remon J, Vervaet C. Near infrared and Raman spectroscopy for the in-process monitoring of pharmaceutical production processes. International Journal of Pharmaceutics. 2011;417(1-2):32-47.

46. Paudel A, Raijada D, Rantanen J. Raman spectroscopy in pharmaceutical product design. Advanced Drug Delivery Reviews. 2015;89:3-20.

47. Tsujimoto H, Yokoyama T, Huang C, Sekiguchi I. Monitoring particle fluidization in a fluidized bed granulator with an acoustic emission sensor. Powder Technology. 2000;113(1-2):88-96.

48. Naelapää K, Veski P, Pedersen J, Anov D, Jørgensen P, Kristensen H et al. Acoustic monitoring of a fluidized bed coating process. International Journal of Pharmaceutics. 2007;332(1-2):90-97.

49. Sheahan T, Briens L. Passive acoustic emission monitoring of pellet coat thickness in a fluidized bed. Powder Technology. 2015;286:172-180.

50. Sheahan T, Briens L. Passive acoustic emissions monitoring of the coating of pellets in a fluidized bed—A feasibility analysis. Powder Technology. 2015;283:373-379.

51. Briens L, Bojarra M. Monitoring Fluidized Bed Drying of Pharmaceutical Granules. AAPS PharmSciTech. 2010;11(4):1612-1618.

52. Daniher D, Briens L, Tallevi A. End-point detection in high-shear granulation using sound and vibration signal analysis. Powder Technology. 2008;181(2):130-136.

53. Hansuld E, Briens L, McCann J, Sayani A. Audible acoustics in high-shear wet granulation: Application of frequency filtering. International Journal of Pharmaceutics. 2009;378(1-2):37-44.

54. Hansuld E, Briens L, Sayani A, McCann J. Monitoring quality attributes for high-shear wet granulation with audible acoustic emissions. Powder Technology. 2012;215-216:117-123.

55. Yu L. Pharmaceutical Quality by Design: Product and Process Development, Understanding, and Control. Pharmaceutical Research. 2008;25(10):2463-2463.

56. Woodcock J. The concept of pharmaceutical quality. American Pharmaceutical Review. 2004;7(60):10–15.

57. Bauer W, Werther J, Emig G. Influence of gas distributor design on the performance of fluidized bed reactor. German Chemical Engineering 1981; 4:291–298.

58. Garncarek Z, Przybylski L, Botterill, J, Broadbent C. A quantitative assessment of the effect of distributor type on particle circulation. Powder Technology. 1997;91:209–216

59. Raich A, Çinar A. Statistical process monitoring and disturbance diagnosis in multivariable continuous processes. AIChE Journal. 1996;42(4):995-1009.

60. MacGregor J, Kourti T. Statistical process control of multivariate processes. Control Engineering Practice. 1995;3(3):403-414.

61. Miletic, I., Quinn, S., Dudzic, M., Vaculik, V. and Champagne, M. (2004). An industrial perspective on implementing on-line applications of multivariate statistics. Journal of Process Control, 14(8), pp.821-836.

62. LeCun Y, Bengio Y, Hinton G. Deep learning. Nature. 2015;521(7553):436-444.

63. LeCun Y, Bottou L, Orr G, Müller K. Efficient BackProp. Lecture Notes in Computer Science. 2012;:9-48.

64. Hinton G, Deng L, Yu D, Dahl G, Mohamed A, Jaitly N et al. Deep Neural Networks for Acoustic Modeling in Speech Recognition: The Shared Views of Four Research Groups. IEEE Signal Processing Magazine. 2012;29(6):82-97.

Chapter 3

In-line Acoustic Monitoring to Determine Fluidized Bed
Performance During Pharmaceutical Coating

3.1 Introduction

Fluidized beds are used to coat pellets or granules containing active pharmaceutical

ingredients. Within a fluidized bed, compressed air is forced into the bottom of a chamber

containing the pellets. Physical drag forces result in a fluidized movement within the

chamber. The coating solution is distributed by an atomizing nozzle positioned either

above or in the pellet bed. Fluidization allows for coating and drying to occur within a

single unit operation. A fluidized bed provides effective mass and heat transfer; however,

as a downside, it can be challenging to operate. The multivariate nature of a fluidized unit

operation can make it challenging to choose optimal process conditions. As suggested by

the pharmaceutical quality by design (QbD) framework, such operating conditions are

inlet air temperature, inlet air flow rate, air dew point, atomizing spray rate, total coating

time, and total drying time (1). Poorly optimized operating conditions can lead to non-

uniform coating, pellet agglomeration, or defluidization; thus, result in unfavorable

production costs from lost material, energy, and time.

The conventional method to monitor process quality is at-line sampling, combined with

weight gain measurement or near infrared spectroscopy (2, 3). Both ways are typically

too slow to be used for real-time process control. Manufacturers and regulators are

looking for the development of innovative Process Analytical Technologies (PAT)s to

monitor fluidized bed conditions that will impact drug quality (4, 5). In 2004, the US

FDA released an extensive guidance document on the topic of new PATs. A useful PAT would be able to reduce manual sampling requirements or complement regular sampling procedures to improve product quality validation or process control.

Several in-line PATs are concurrently being investigated for fluidized bed application. Automated digital imaging was demonstrated as a technology to monitor pellet growth (6). High speed images recorded using a light source and optical detector placed inside the fluidized bed can be combined with image processing and statistical analysis to provide real-time feedback of coating conditions and agglomerate formation inside the equipment. However, imaging techniques require a window or lens into the fluidized bed. These windows frequently become fouled by the coating solution and result in inaccurate readings. Similar field of view challenges are faced using in-line near-infrared spectroscopy (7, 8).

Microwave resonance technology has been proposed as an option for measuring drying rate during fluidized bed granulation (9, 10). An electromagnetic field is used to adjust the dipole moments of water molecules within the fluidized bed. Upon releasing the field, a change in energy is detected. The magnitude of this change in system energy can be related to the moisture content remaining inside the process equipment. This method of production monitoring is very promising; however, would be expensive to implement relative to the other techniques discussed.

Naelapää et al. demonstrated the extraction of process information from passive acoustic emissions recorded during fluidized bed coating of potassium chloride crystals with ethylcellulose. Although the data did not fully support their hypothesis, the trials

established a possibility for passive acoustic emissions monitoring in fluidized bed process control applications. Naelapää et al. further recommended that acoustic detectors with an upper frequency of 16.5 kHz were less effective than detectors with a high frequency of 50 kHz (11). Tsujimoto et al. studied in-line monitoring of high-frequency elastic waves between 100 kHz - 140 kHz for pharmaceutical fluidized bed applications (12). Investigation at these frequencies can provide the benefit of highly localized monitoring data; however, prolonged continuous recording at high frequencies will result in excessive data generation and computer processing requirements.

Sheahan and Briens recently studied passive acoustic emissions monitoring at 40 kHz while coating glass pellets in a fluidized bed (13, 14). This feasibility study demonstrated that microphones placed external to a fluidized bed can effectively detect transitions between coating and drying stages of operation. The research provided insight towards the application of passive acoustic emissions monitoring in pharmaceutical manufacturing; however, was limited to a single set of operating conditions. Additional research is required to build upon this feasibility study and understand how adjusting process variables (such as fluidization air temperature or aqueous coating material) will affect the passive acoustic emissions recordings.

The current study was designed to build upon Sheahan and Briens feasibility studies, and further investigate changes in passive acoustic emissions during fluidized bed coating. It was understood that application of a coating would degrade the fluidized bed hydrodynamics, and thus should affect the sound waves generated during pellet collisions. Drying would subsequently reverse these changes in bed hydrodynamics. Changes in the process between independent coating trials at three temperatures ($20^{o}C$,

40°C, and 56°C) were considered to determine the effects on the acoustic emissions. It was hypothesized that increasing the bed temperature would increase the drying rate of the wet coated pellets and that this controlled change would be detected in the passive acoustic emissions. The rate of signal change could then be extracted as a validation of drying efficiency.

3.2   Materials and Methods

3.2.1   Pellets

Spherical 1000 μm glass pellets were used for the experiments. These pellets were used as a model for pharmaceutical pellets such as Cellets® or Suglets®. Glass pellets are reusable, experience low friability, and provide similar shape and diameter as pharmaceutical pellets; however, they have a higher density (2400 kg/m^3) than Suglets® (2043 kg/m^3) and Cellets® (1800 kg/m^3). Various pellet models will influence the sound amplitude and frequency; however, the fundamental signal trends should remain the same. Batch size for each fluidized bed trial was 2 kg.

3.2.2   Coating Material

A 5% (w/w) sugar water solution was used in the initial coating trials. Sugar-based coatings can be applied in drug manufacturing to mask API taste. A 5% (w/w) Acryl-EZE® water solution was also used to compare against the sugar coating trials. Functional polymer coatings, such as Acryl-EZE®, are frequently used to adjust release profiles.

3.2.3   Fluidized bed

The pellets were fluidized in a conical top spray fluidized bed. Figure 3.2 illustrates the equipment and its dimensions. Compressed air was passed through a Dutch weave distributor plate at the base of the bed into the pellet chamber. Four bag filter exhaust outlets were located at the top of the chamber. Relative air humidity remained near 9%. The superficial gas velocity throughout the fluidized bed was regulated to 1.7 m/s (3.1x the minimum fluidization velocity). Fluidization air temperature was set to either 20°C, 40°C, or 56°C using a t-type process air heater.
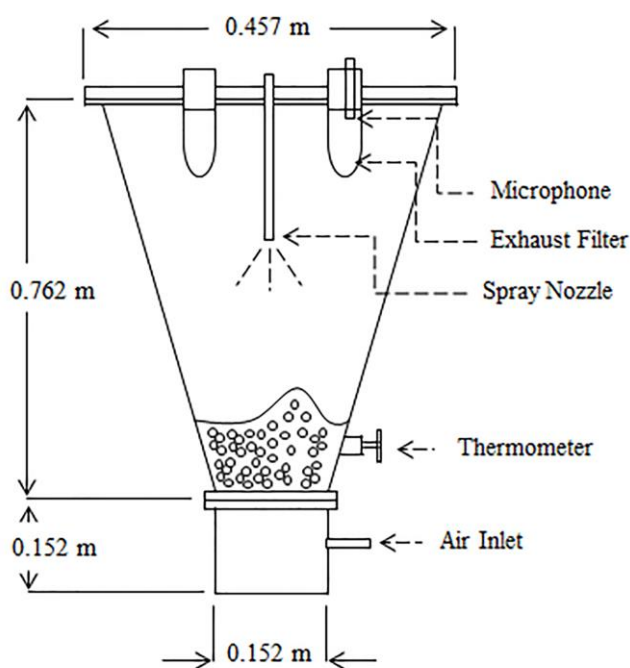
Figure 3.1 Schematic of the fluidized bed identifying microphone placement

3.2.4 Coating Process

An atomizing spray nozzle (John Brooks Company 1/8 PRJJB 0.0390) was inserted 0.56 m above the distributor plate. The pellets were sprayed four times with the coating

solution for two-minute intervals during the 80-minute process. A total of 208 ml of coating solution was applied at a rate of 26 mL/min during each trial. The bed remained fluidized between coating applications to allow for adequate pellet drying. The length of each drying stage was predetermined through prior experiments. Without adequate drying time, excessive coating buildup resulted in bed defluidization. The drying stages increased from 6, 12, 16, and finally 26 minutes during each trial.

3.2.5   Data Acquisition

A PCB Piezotronics 130D10 microphone with attached 130P10 preamplifier was placed within the exhaust. The microphone recorded at a rate of 40 kHz. This allowed for analysis within the audible below 20 kHz. For data acquisition, a 16-bit National Instruments DAQCard-6036E was used. Signal processing was completed in MATLAB R2016b.

3.2.6   Drying Tunnel

250 g samples of the glass pellets were mixed with either a 5% (w/w) sugar water solution or 5% (w/w) Acryl-EZE® water solution and placed in a drying tunnel at specified temperatures (20ºC, 40ºC, and 56ºC). The change in mass of the pellets over time was recorded to determine drying rates. These drying rates were compared to information obtained from the passive acoustic emissions from the fluidized bed

3.2.7   Flow Analysis

A Mercury Scientific Revolution Powder Analyzer was used to measure the changes in flowability of glass beads coated in either 5% (w/w) sugar water or 5% (w/w) Acryl-

EZE® water solution between 0-20% moisture content. Avalanche time was calculated based on an average of 50 measured data points. Shorter avalanche times indicate higher bulk flowability.

3.2.8   Coefficient of Restitution

The coefficient of restitution was measured to highlight the changes in elastic energy between three states: clean uncoated pellets, wet coated pellets, and coated pellets that have been fully dried. The measurement method was similar to that used by Muller et al. (15). A piezoelectric microphone was attached to the surface of a horizontal metal plate. The pellets were dropped into a free fall and bounced on the plate until coming to rest. Each impact was recorded using the microphone. The ratio of time between successive rebounds was used to determine the coefficient of restitution at clean, wet coated, and dry coated states.

3.3   Results

3.3.1   Coating Process

Visual observations from the viewing window of the bed verified that the pellets remained fluidized. The fluidization profile could be described as spouted, with distinct air pockets moving vertically through the pellets. Samples were removed following the 40°C trials and imaged using a Hitachi S-4500 field emission scanning electron microscope at 3.00 kV. Samples were coated with gold to enhance conductivity before imaging. These images, as shown in Figure 3.2, validated that a film was successfully applied and coated the pellets during the 80-minute trial.
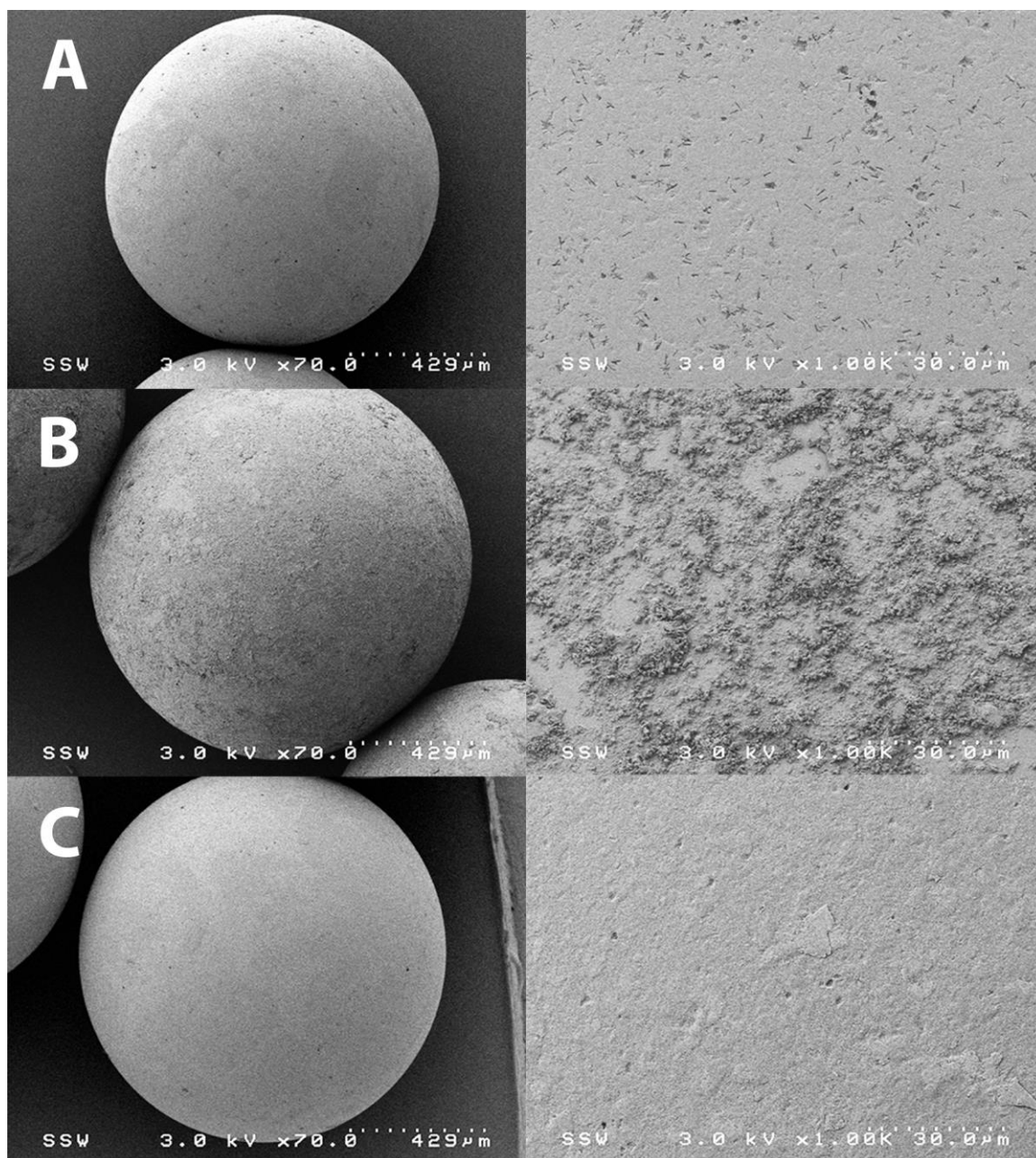
Figure 3.2 Scanning electron microscope images of pellets without coating (A), with sugar coating (B), and with Acryl-EZE® coating (C)

3.3.2   Passive Acoustic Emissions

Acoustic emissions were analyzed in MATLAB R2016b. Figure 3.3 shows the raw data during a coating trial at 40ºC.
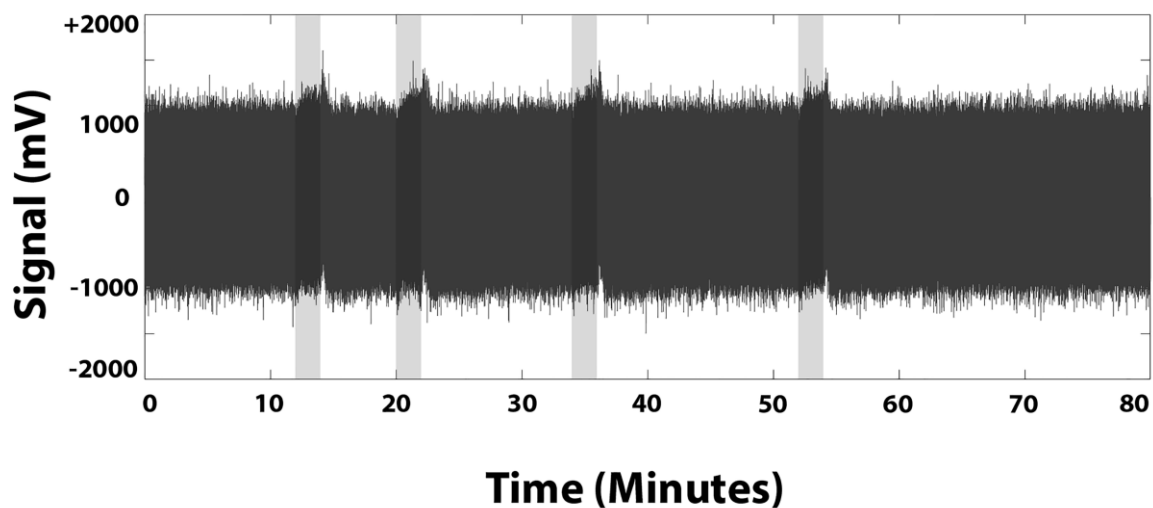
Figure 3.3 Unfiltered acoustic emissions during Acryl-EZE® coating trial at 40ºC. The vertical grey bars identify each two-minute spray coating stage

As shown in Figure 3.4, a moving standard deviation filter was applied to enhance changes in the data. To reduce signal noise, a Savistzky-Golay filter was applied to the remaining data set. During each spraying stage, the standard deviation of the signal increased by approximately 40 mV. During the drying stages, the standard deviation of the signal decreased linearly.
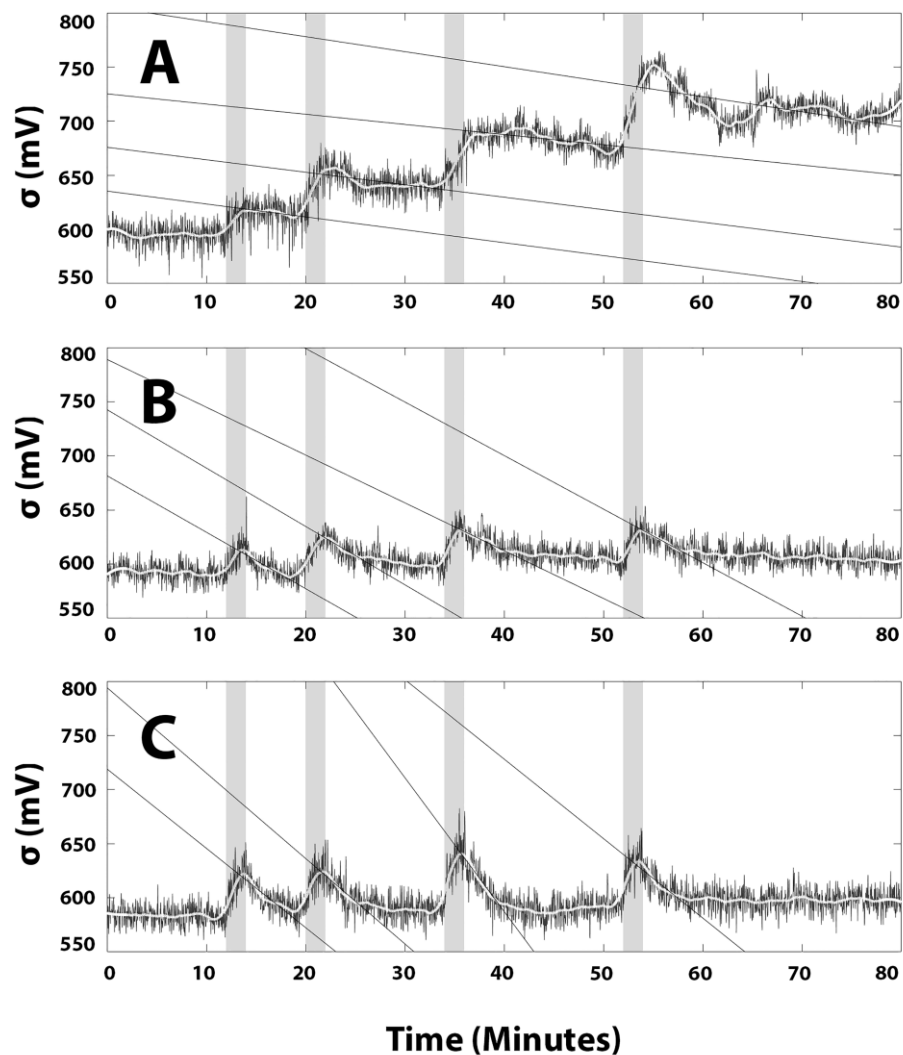
Figure 3.4 Standard deviation (σ) of acoustic emissions during sugar coating trials at 20°C (A), 40°C (B), and 56°C (C).

It was observed that the rate of signal change ($d\sigma/dt$) during the drying stages was higher while operating at higher temperatures. As shown in Figure 3.4, the passive acoustic emissions during drying at 20°C changed by an average rate of - 1.17 mV/min (R^2 = 0.49), while the signals during the 40°C and 56°C trials changed at - 4.99 mV/min (R^2 = 0.95), and - 7.52 mV/min (R^2 = 0.91) respectively.

Figure 3.5 shows the drying rates of 250 g glass bead samples coated in a 5% (w/w) sugar water solution, as measured independently in a drying tunnel. The change in moisture concerning time (dM/dt) was highest at 56°C, lower at 40°C and substantially lower at 20°C at rates of - 0.034 wt%/min, - 0.12 wt%/min, and - 0.189 wt%/min respectively. These rates were comparable with the fluidized bed recovery as measured using passive acoustic emissions as shown in Figure 3.6.
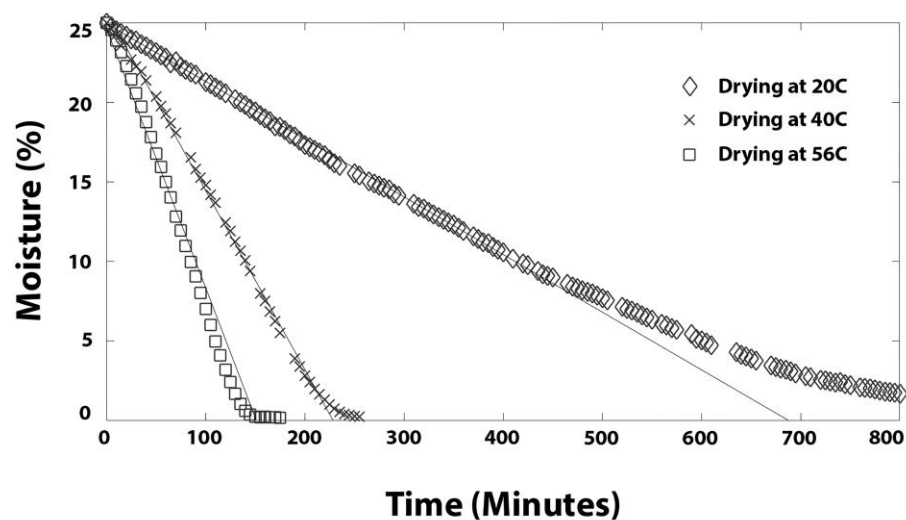
Figure 3.5 Drying curve glass pellets observed in a drying tunnel at 20°C, 40°C, and 56°C after being coated in a 5% (w/w) sugar water solution
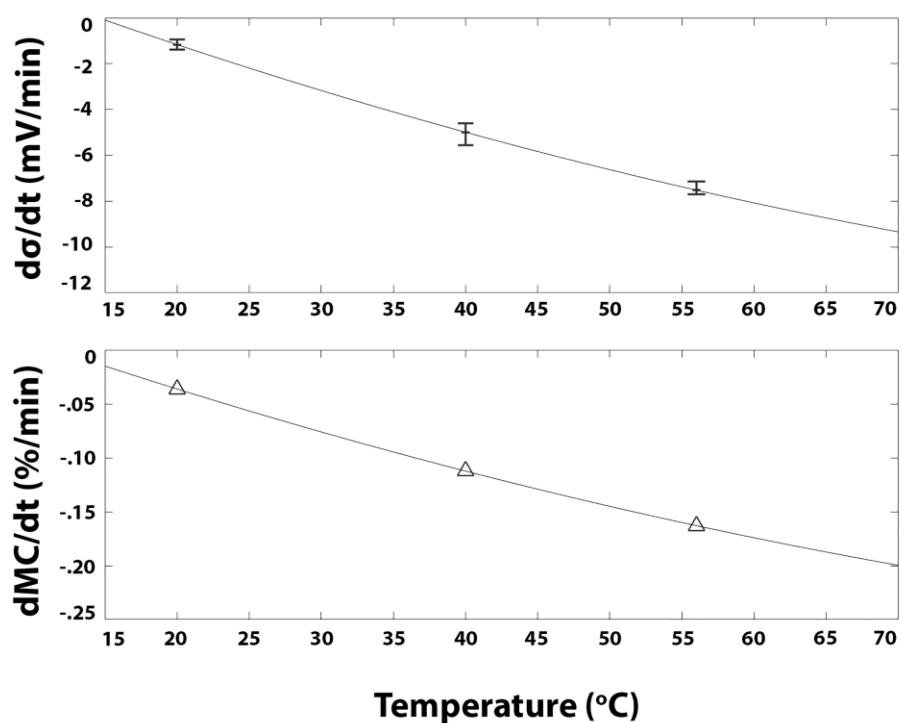
Figure 3.6 Acoustic signal change during each drying stage of sugar coating trials at compared against drying rate observed in a drying tunnel

In the final trial, an aqueous Acryl-EZE® polymer coating was applied onto the glass pellets at 40°C. The data was compared with the sugar coating trial at the same temperature as shown in Figure 3.7. The rate of signal change ($d\sigma/dt$) during each of the drying stages were similar: - 5.57 mV/min ($R^2 = 0.95$) for the Acryl-EZE® coating compared to - 4.99 mV/min ($R^2 = 0.95$) for the sugar coating.
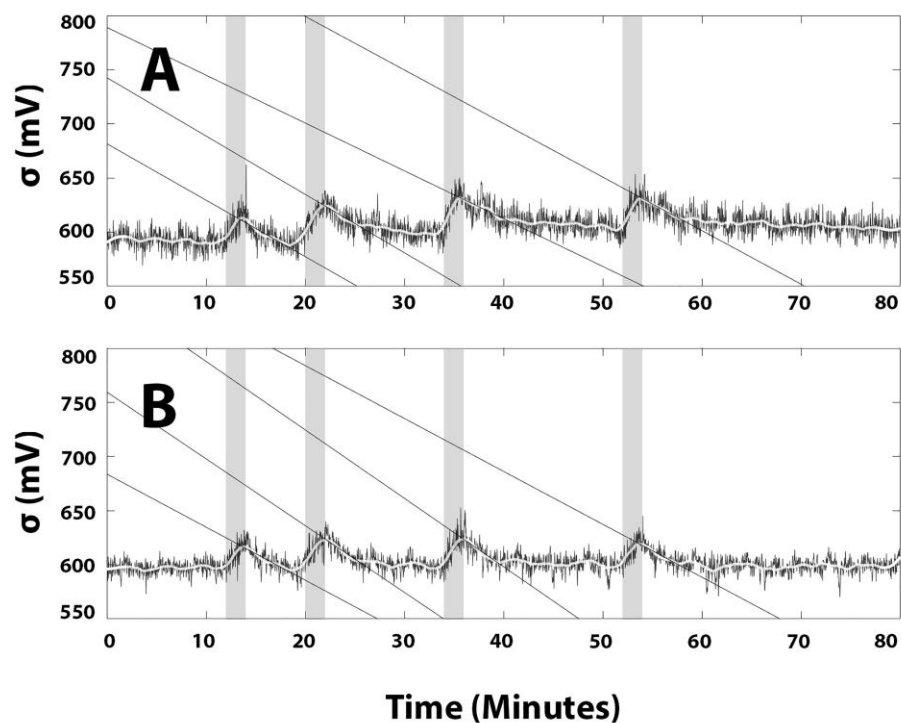
Figure 3.7 Standard deviation (σ) of acoustic emissions during fluidized bed sugar coating trial at 40°C (A) and Acryl-EZE® coating trial at 40°C (B).

The comparable trends between sugar coating and Acryl-EZE® coating were supported using independent drying, flowability, and coefficient of restitution data. Figure 3.8 shows that pellets coated in either sugar or Acryl-EZE® experienced similar drying profiles inside a controlled drying tunnel environment. Figure 3.9 shows that pellets coated in either sugar or Acryl-EZE® underwent similar flowability changes based on avalanche data at various moisture contents. Figure 3.10 shows that pellets coated in either sugar or Acryl-EZE® underwent similar changes in their coefficients of restitution when coated.
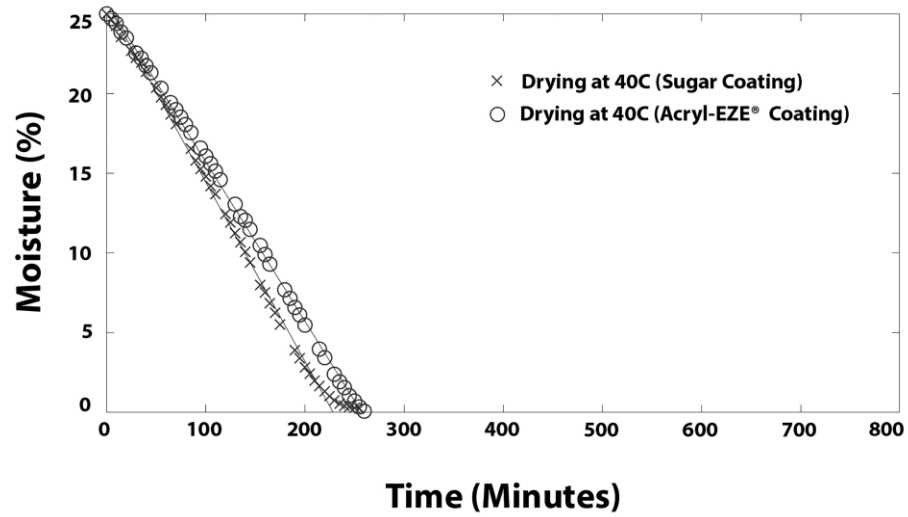
Figure 3. 8 Drying curve for glass pellets observed in a drying tunnel at 40°C after being coated in either 5% (w/w) sugar water or 5% (w/w) Acryl-EZE® water
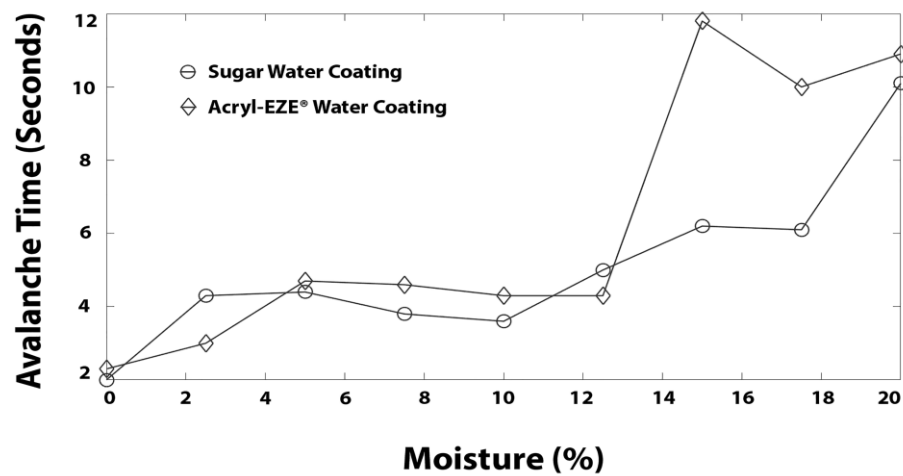
Figure 3.9 Flowability of pellets measured as avalanche time (seconds) between 0 – 20% moisture content coated in either 5% (w/w) sugar water or 5% (w/w) Acryl-EZE® solutions
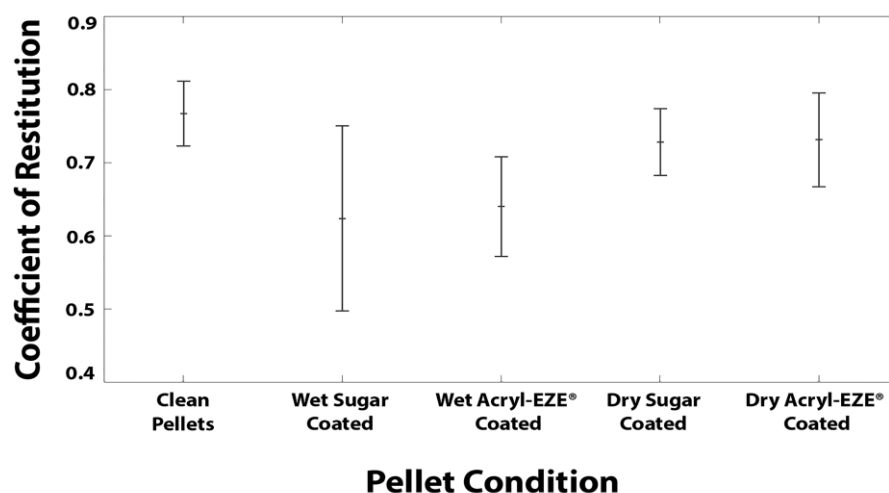
Figure 3.10 Coefficient of restitution recorded from clean uncoated pellets, wet coated pellets, and coated pellets that have been thoroughly dried using both 5% (w/w) sugar water or 5% (w/w) Acryl-EZE® solutions

3.4   Discussion

Passive acoustic emissions from fluidization are classified based on three independent sources (15). Impact sound originates from particle-particle and particle-chamber collisions within the bed. Friction sound arises from particle-particle contact as they pass one another. Aerodynamic sound originates from air movement. Sound waves generated by each of these sources disperse through the equipment boundaries. Sheahan and Briens previously demonstrated that a piezoelectric microphone recording at 40 kHz can detect real-time changes from within the fluidized bed (13, 14). Further research was required to build upon their feasibility study and demonstrate how PAE monitoring can be linked to specific process variables.

The moving standard deviation of the PAEs increased by 40 mV during each coating stage and then decreased during each drying stage (Figure 3.4). As the pellets dry, the

elastic properties of all pellets within the fluidized bed become uniform and acoustic variability decreases. Higher operating temperatures increase the vapor pressure of the liquid film on the pellet surfaces. This increases the driving force for drying. The changes in drying rate were monitored using the passive acoustic emissions. At higher temperatures, the signal recovered at a faster rate: - 1.17 mV/min at 20°C, - 4.99 mV/min at 40°C, and - 7.52 mV/min at 56°C.

Figure 3.4A shows that the standard deviation of the acoustic emissions for the trial at 20°C did not wholly recover during the drying phase to the pre-spray level. The fluidization air temperature was too low to dry the coating effectively. Based on visual observation, approximately 20% of the pellets had formed into agglomerates ranging from 0.5 – 5 cm diameter at the end of the 20°C trial. Very few agglomerates were found during the 40°C and 56°C trials. However, higher temperatures are less economical from a process energy management standpoint. Excessively heating the fluidization air stream for extending drying periods isn't cost-effective or environmentally considerate. The methods presented in this research to monitor production using passive acoustics could, in practice, support determination of an optimal drying temperature: high enough to prevent defluidization, and low enough to conserve energy.

Figure 3.7 compares the monitoring results from a trial using sugar-based coating against a trial using Acryl-EZE® coating. The coating volume and spray pattern were identical in each trial. The PAE monitoring results were similar: an increase during spraying (reflecting higher cohesivity of the wet pellets and their nonuniform distribution in the bed) followed by a decrease during drying (as the pellets dry to improve fluidization quality). The increase in the standard deviation was approximately the same for both

coating solutions. The rate of decrease was also similar for both solutions. The findings were supported from the independent drying measurements (Figure 3.8), flowability measurements (Figure 3.9), and coefficient of restitution data (Figure 3.10).

The coefficient of restitution for a pellet decreases as it is covered with a wet solution (Figure 3.10). The collisions between wet pellets are less elastic, resulting in energy dissipation. This dissipated energy decreases the energy transmitted to the microphone, resulting in lower amplitude of measured acoustics. As the coating solution is applied, the top layer of pellets becomes wet, while the pellets lower in the bed remain dry until adequate mixing occurs. There is an initial distribution of pellets with varying amounts of coating. The wet coating solution: (a) adds some mass to a pellet thereby slightly reducing its velocity within the bed; the energy transferred with a collision may be affected depending on the ratio of mass added versus velocity reduced which affects the energy recorded by a microphone (b) increases the cohesivity of the pellets such that pellet agglomerates with more mass but less velocity may form; this change in particulate properties can affect the energy recorded from collisions (c) reduces the coefficient of restitution as the coating solution makes the collision less elastic, lowering the energies recorded by a microphone.

5.   Conclusions

This research investigated passive acoustic emissions monitoring for fluidized bed pellet coating processes. First, this study verified that distinct shifts in passive acoustic emissions could differentiate between coating and drying stages inside the fluidized bed. Second, this study identified that changes in drying rate (controlled by fluidizing air

temperature) can be extracted from the acoustic emissions. And finally, it was observed that acoustic emission profiles were similar while using different coating solutions.

Due the complexity of the system, uncontrolled variables may have played a secondary role influencing the microphone signal. As example, filter blockage from coting droplets that rise upwards into the exhaust would gradually shield the microphone from acoustic emissions in the chamber. These uncontrolled interactions were considered minor experimental uncertainties and are not expected to have played a significant role in the drying trends extracted from the acoustic data.

Overall, extracted information from passive acoustic emissions can contribute to the real-time monitoring strategy of a fluidized bed pellet coating process. A more comprehensive monitoring strategy would aid in reliable identification of process disruptions. Parameters, such as air temperature, can then be quickly adjusted to recover and regain optimal operation. This non-intrusive monitoring method is robust, adaptable, and can easily be implemented with various manufacturing systems.

3.6   References

1. Yu L. Pharmaceutical Quality by Design: Product and Process Development, Understanding, and Control. Pharmaceutical Research. 2008;25(10):2463-2463.

2. Naidu V, Deshpande R, Syed M, Deoghare P, Singh D, Wakte P. PAT-Based Control of Fluid Bed Coating Process Using NIR Spectroscopy to Monitor the Cellulose Coating on Pharmaceutical Pellets. AAPS PharmSciTech. 2016;18(6):2045-2054.

3. Kirsch J, Drennen J. Near-infrared spectroscopic monitoring of the film coating process. Pharmaceutical Research. 1996;13(2):234-237.

4. U.S. Department of Health and Human Services Food and Drug Administration. Guidance for Industry PAT — A Framework for Innovative Pharmaceutical Development, Manufacturing, and Quality Assurance. 2004

5. Hinz D. Process analytical technologies in the pharmaceutical industry: the FDA's PAT initiative. Analytical and Bioanalytical Chemistry. 2005;384(5):1036-1042.

6. Možina M, Tomaževič D, Leben S, Pernuš F, Likar B. Digital imaging as a process analytical technology tool for fluid-bed pellet coating process. European Journal of Pharmaceutical Sciences. 2010;41(1):156-162.

7. Lee M, Seo D, Lee H, Wang I, Kim W, Jeong M, et al. In line NIR quantification of film thickness on pharmaceutical pellets during a fluid bed coating process. International Journal of Pharmaceutics. 2011;403(1-2):66-72.

8. Marković S, Poljanec K, Kerč J, Horvat M. In-line NIR monitoring of key characteristics of enteric coated pellets. European Journal of Pharmaceutics and Biopharmaceutics. 2014;88(3):847-855.

9. Buschmüller C, Wiedey W, Döscher C, Dressler J, Breitkreutz J. In-line monitoring of granule moisture in fluidized-bed dryers using microwave resonance technology. European Journal of Pharmaceutics and Biopharmaceutics. 2008;69(1):380-387.

10. Lourenço V, Herdling T, Reich G, Menezes J, Lochmann D. Combining microwave resonance technology to multivariate data analysis as a novel PAT tool to improve process understanding in fluid bed granulation. European Journal of Pharmaceutics and Biopharmaceutics. 2011;78(3):513-521.

11. Naelapää K, Veski P, Pedersen J, Anov D, Jørgensen P, Kristensen H et al. Acoustic monitoring of a fluidized bed coating process. International Journal of Pharmaceutics. 2007;332(1-2):90-97.

12. Tsujimoto H, Yokoyama T, Huang C, Sekiguchi I. Monitoring particle fluidization in a fluidized bed granulator with an acoustic emission sensor. Powder Technology. 2000;113(1-2):88-96.

13. Sheahan T, Briens L. Passive acoustic emission monitoring of pellet coat thickness in a fluidized bed. Powder Technology. 2015;286:172-180.

14. Sheahan T, Briens L. Passive acoustic emissions monitoring of the coating of pellets in a fluidized bed—A feasibility analysis. Powder Technology. 2015;283:373-379.

15. Müller P, Trüe M, Böttcher R, Tomas J. Acoustic evaluation of the impact of moist spherical granules and glass beads. Powder Technology. 2015;278:138-149.

Chapter 4

An Application of Deep Learning to Detect Process Upset during Pharmaceutical Manufacturing using Passive Acoustic Emissions

4.1   Introduction

4.1.1   Fluidized Bed Blockage

Within a fluidized bed, air is introduced through a distributor plate located at the bottom

of a conical chamber. The moving air is used to continuously mix and dry material that

has been placed inside the chamber. Past studies have related distributor plate design to

bubble size and radial gas distribution as an assessment of fluidization quality (1, 2).

Recently, Wormsbecker and Pugsley studied fluidized bed pressure changes through

spectral analysis to determine dominant bubble frequencies and subsequently related

these frequencies to distributor plate performance for granule drying (3). Common

distributor plate designs include perforated plates, punched plates, or Dutch weave plates.

The relatively small bubbles formed by Dutch weave distributor plates exhibit higher risk

of defluidization while operating at low air velocities (3).

During fluidized bed pellet coating applications, distributor plate blockage can occur

between the coating and drying stages. For example, agglomerated pellets can settle on

the distributor plate or the distributor plate can become blinded by the coating solution.

As the aqueous coating solution is applied to the bed, small liquid bridges form between

pellets. If the kinetic energy provided by fluidization is inadequate, and the liquid bridge

between two pellets solidifies, an agglomerate will form (4). The agglomerated pellets

require larger upward forces to remain fluidized and tend to settle onto the distributor plate. If multiple pellets settle along one edge of the distributor plate, the significant blockage will begin to shift inlet airflow to the opposite side and increase the likelihood of additional agglomerate formation in the void space above the blockage. On the other hand, a blinding of the distributor plate will occur under conditions of excessive spray and inadequate drying. As coating solution is applied to the bed, a fraction of the spray will build up along the walls of the chamber. This build-up of excess solution will tend to drip down the wall and blind off the distributor plate in an annular pattern along its edges. This blinding gradually moves towards the center of the distributor plate. Both blockage patterns will have a substantial impact on product quality. Inconsistent hydrodynamics between batches will result in product variability. Failed quality assurance will lead to lost material and higher operating costs.

4.1.2   Passive Acoustic Emissions

Passive acoustic emission monitoring has shown potential as a technology to monitor the fluidized bed coating processes. Sheehan and Briens demonstrated that signals recorded using piezoelectric microphones attached to the wall and placed within the air exhaust of a fluidized bed during coating application can provide distinct signal shifts that correspond to physical process changes (5,6). These microphones actively record acoustic emissions within the audible range and can act as a basis for the development of process analytical techniques to improve control. Further work is required to expand on this feasibility study. Research is needed to understand how undesirable process failures will affect the acoustic signals, and if control strategies can be developed based on

information obtained from the passive acoustics. Difficulty in extracting valuable process information is one explanation to why acoustic monitoring remains uncommon in industry today (7). With advances in computer processing, the analysis of high frequency data sets over extended study times is no longer a challenge.

4.1.3   Deep Learning

Deep learning was a topic of interest through the 1980s; however, limitations in computing diminished any widespread societal or industrial adoption (8, 9, 10). Breakthroughs in parallel processing within the last decade have started to revive the study. This sudden revival has led to the development of highly efficient artificial intelligence computing systems that are capable of multivariate data manipulation. Deep neural networks have been proven to solve extreme data problems, such as classifying features within images (8, 9) or discovering genetic determinants of disease (10).

A deep learning program is modeled after the human brain. The network receives raw input data that is analogous to our sensory neurons. The network then processes this data through a "hidden layer" that determines the data's significance. The program can be trained to classify and make decisions regarding future inputs based on its prior learning.

For the present study, experiments were developed to simulate various fluidized bed distributor plate blockages. Segmented and annular shaped blockages were introduced while acoustic emissions were recorded. As the blockage increased, the air velocity into the bed consequently increased. It was hypothesized that, at higher air velocities, the

pellet-pellet and pellet-wall impact energy would increase, thus affecting the acoustic emissions being recorded. The experiments used both 1000 μm diameter glass pellets and 1000 μm Suglets® pellets to assess the effect of pellet density.

4.2   Materials and Methods

4.2.1   Fluidized bed

Pellets were fluidized inside a top spray fluidized bed as shown in Figure 4.1. Microphones were placed inside an exhaust filter and securely attached externally onto the wall of the conical chamber.
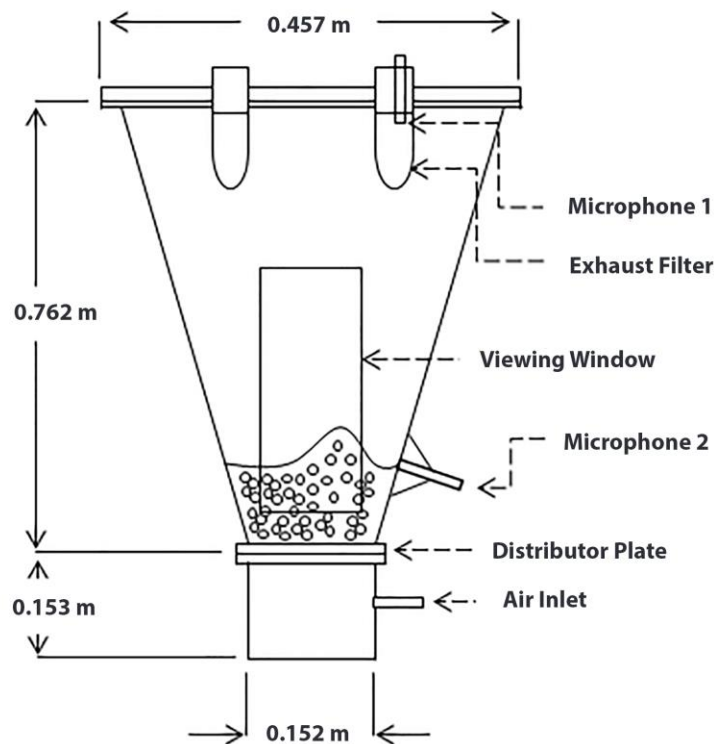

Figure 4.1 Fluidized bed schematic identifying microphone placement

A large glass viewing window allowed for visual observations of bed dynamics during each trial. The distributor plate had a Dutch weave design allowing air to flow through small curved triangles between the mesh. The Dutch weave design provides high radial dispersion of very small bubbles but can be more susceptible to localized defluidization while operating at low flowrates (3). This drawback suggested that the Dutch weave distributor plate design would be relevant for distributor plate blockage studies.

4.2.2   Pellets

Spherical 1000 μm Suglets® and 1000 μm glass pellets were used for the experiments. Suglets® (2043 kg/m^3) are small sugar spheres commonly used as non-pareil particles in drug manufacturing processes. Glass pellets (2400 kg/m^3) of the same size were used as a model to compare the effect of pellet density. The glass pellets are consistent in sphericity and do not experience any friability inside the chamber. Fluidization air flow into the bed was set to 0.028 m^{3}s^{-1} for trials using Suglets® pellets. To achieve a comparable Geldart D fluidization profile (11) using glass pellets, air flowrate was increased to 0.032 m^{3}s^{-1}. The relationship was determined by pellet density, Ergun's equation for fluid flow through packed columns (12), and Wen's correlation to approximate voidage (13).

4.2.3   Distributor Plate Obstruction

For each experiment, sections of the distributor plate were blocked off using high strength tape as shown in Figures 4.2 and 4.3. The corresponding changes in gas velocity entering the bed are also indicated. The segmented blockage was designed to simulate the

accumulation of agglomerated pellets on the plate. The annular blockage was intended to simulate blinding of the plate by the coating solution.

Segmented Blockage						
Blockage Area (%)	4.0	11.0	19.6	29.2	39.4	50.0
Air Velocity (m/s) Glass Pellets	1.94	2.09	2.32	2.63	3.08	3.73
Air Velocity (m/s) Sugar Pellets	1.60	1.72	1.91	2.17	2.53	3.07

Figure 4.2 Segmented distributor plate blockage patterns with blockage area and air velocity

Annular Blockage						
Blockage Area (%)	16.0	30.5	43.8	55.6	66.0	75.0
Air Velocity (m/s) Glass Pellets	2.22	2.68	3.31	4.19	5.48	7.46
Air Velocity (m/s) Sugar Pellets	1.83	2.21	2.73	3.45	4.51	6.14

Figure 4.3 Annular distributor plate blockage patterns with blockage area and air velocity

4.2.4   Passive Acoustic Data Acquisition

Piezoelectric microphones were placed within the exhaust and securely attached externally to the wall of the fluidized bed chamber. The wall microphone was located away from the segmented blockages on the opposite side of the chamber. All passive acoustic emissions were recorded at 40 kHz to support the constrains of Nyquist sampling theorem while analyzing the signal inside the limits of audible range frequencies. MATLAB and Python were used offline for signal filtering and analysis.

4.2.5   Deep Learning

The artificial neural network was designed to classify upset conditions from a bulk data array of audio feature vectors. No prior knowledge was required concerning the importance of the individual features; instead, the network's purpose was to look at all features and distinguish their significance through parallel cost function evaluation and back propagation. The 34 time and frequency domain vectors were extracted using pyAudioAnalysis open source library (14). The bulk extraction included features such as zero crossing rate, energy, spectral flux, and mel-frequency cepstral coefficients which are typically used by the deep learning community for voice or music classification.

The network's design was completed in Python using the Theano library (15) for efficient computations. TensorFlow^{TM} (16) was used to run the deep learning application with the support of the Keras (17) library for efficient coding. The network was composed of one input layer, two hidden layers, and one output layer. The input layer contained 34 feature vectors which were extracted from 0.25 second segments of the acoustic emissions. Each

of the two hidden layers included 22 nodes which were activated using the rectifier

function. The output layer contained 7 nodes that corresponded to the 6 blockage

conditions, and the unblocked reference condition (Figure 4.4). The output layer was

activated using the SoftMax function. Backpropagation took place using 100 epochs

based on initial model optimization.
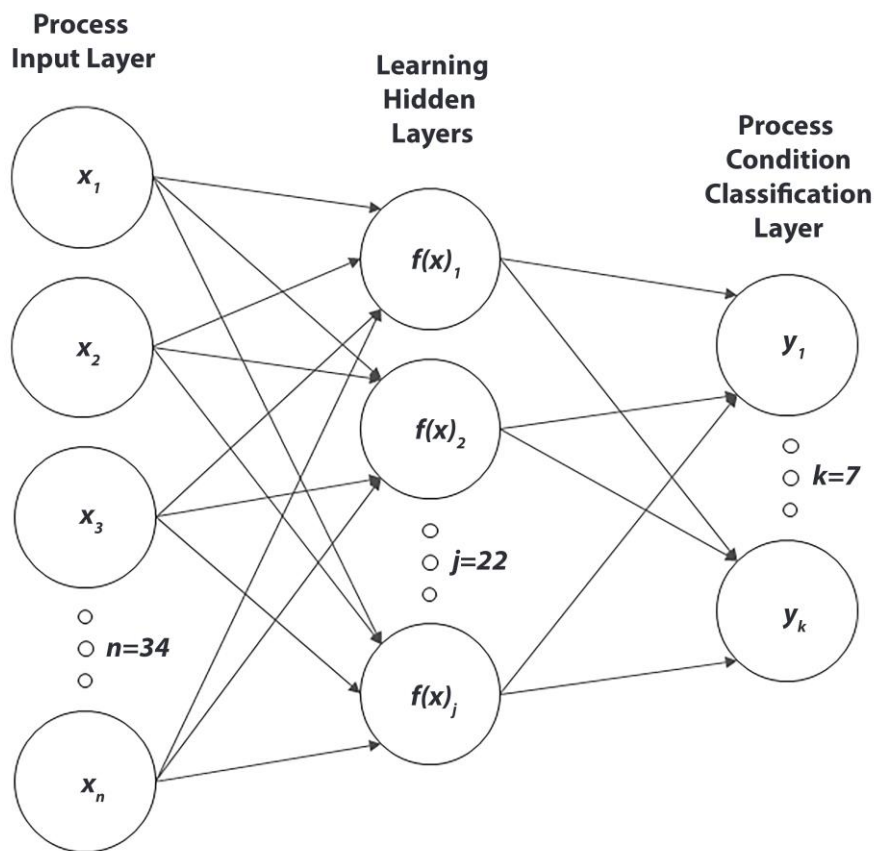
Figure 4.4 Deep learning schematic identifying inputs, outputs, and hidden layers

4.3   Results

Blockages were simulated by actively covering areas of the distributor plate. The project's success depended on the artificial neural network's ability to classify each increasing blockage size within reasonable accuracy. It was observed through the viewing window that pellet velocity and bed hydrodynamics shifted during each trial. As the blockage increased, pellets spouted higher into the freeboard.

Each independent recording was cut into 240 equal segments of 0.25 second length and analyzed using pyAudioAnalysis for short-term time and frequency domain feature extraction. The feature vectors were combined into a data set and labelled by corresponding blockage condition. The data set was split into a training group and test group. Data was analyzed independently for the two blockage types, two microphones, and two pellet materials (Figures 4.5 – 4.7).

Figure 4.5 shows the glass pellet prediction results in an error matrix. Most of the artificial neural network predictions fell on the correct classification, with incorrect predictions typically falling to neighboring blockage sizes. Just 0.17% of the predictions at the maximum blockage size provided a false-negative outcome. Figure 4.6 shows the Suglets® sugar pellet results in an error matrix.

Glass Pellets

Annular Blockage Exhaust Microphone

	0%	16%	31%	44%	56%	66%	75%
0%	242	64	17	0	0	0	0
16%	75	215	45	0	0	0	0
31%	17	28	266	2	0	0	0
44%	0	0	2	270	54	7	0
56%	0	0	0	28	268	26	3
66%	0	0	0	3	41	309	37
75%	0	0	0	0	0	9	314

Annular Blockage Wall Microphone

	0%	16%	31%	44%	56%	66%	75%
0%	269	45	4	4	0	0	0
16%	9	315	13	0	2	0	0
31%	1	57	283	2	0	0	0
44%	0	1	1	291	21	1	1
56%	0	0	1	14	294	7	6
66%	0	0	2	2	16	325	24
75%	0	0	0	1	5	12	313

Segmented Blockage Exhaust Microphone

	0%	4%	11%	20%	29%	39%	50%
0%	296	24	3	2	0	0	0
4%	53	214	46	21	0	0	0
11%	4	32	207	73	15	1	0
20%	2	8	49	238	31	3	0
29%	0	0	18	48	211	30	5
39%	0	0	2	7	47	296	25
50%	0	0	0	0	8	46	282

Segmented Blockage Wall Microphone

	0%	4%	11%	20%	29%	39%	50%
0%	263	19	14	15	11	0	2
4%	53	209	34	39	9	2	0
11%	12	53	209	41	21	10	1
20%	14	17	29	180	35	15	7
29%	7	8	7	40	241	27	13
39%	2	1	6	10	50	235	61
50%	2	2	1	4	22	38	254

Figure 4.5 Error matrix of test set predictions for glass pellets

SUGLETS® Sugar Pellets

Annular Blockage Exhaust Microphone

	0%	16%	31%	44%	56%	66%	75%
0%	240	49	36	0	0	0	0
16%	138	134	56	0	0	0	0
31%	45	39	242	3	0	0	0
44%	1	0	0	312	18	0	0
56%	0	0	0	17	308	13	0
66%	0	0	0	0	23	309	29
75%	0	0	0	0	0	11	323

Annular Blockage Wall Microphone

	0%	16%	31%	44%	56%	66%	75%
0%	309	6	4	2	3	0	0
16%	15	313	9	8	1	0	0
31%	3	10	329	0	1	1	3
44%	5	9	0	276	2	4	1
56%	4	3	2	6	318	6	4
66%	0	1	1	1	7	340	15
75%	0	0	0	1	0	10	312

Segmented Blockage Exhaust Microphone

	0%	4%	11%	20%	29%	39%	50%
0%	191	101	26	5	0	0	0
4%	96	165	43	28	2	1	0
11%	23	60	155	57	17	1	0
20%	8	45	88	136	52	4	0
29%	0	2	21	31	211	55	5
39%	0	1	0	4	82	203	100
50%	0	0	0	0	7	42	274

Segmented Blockage Wall Microphone

	0%	4%	11%	20%	29%	39%	50%
0%	252	16	16	14	16	7	3
4%	8	291	12	9	5	7	7
11%	9	20	223	47	22	15	4
20%	6	11	13	252	8	5	4
29%	6	1	4	7	287	33	3
39%	0	4	5	4	31	302	12
50%	2	6	2	3	9	29	292

Figure 4.6 Error matrix of test set predictions for sugar pellets

The lower density sugar pellets provided similar monitoring results as the glass. In Figure 4.6, the contrasting performance between the exhaust and wall microphones becomes more visible. The exhaust microphone's error rate was highest during small blockage sizes but improved as blockage size increased. Figure 4.7 shows the accuracy results using 10-fold cross validation.
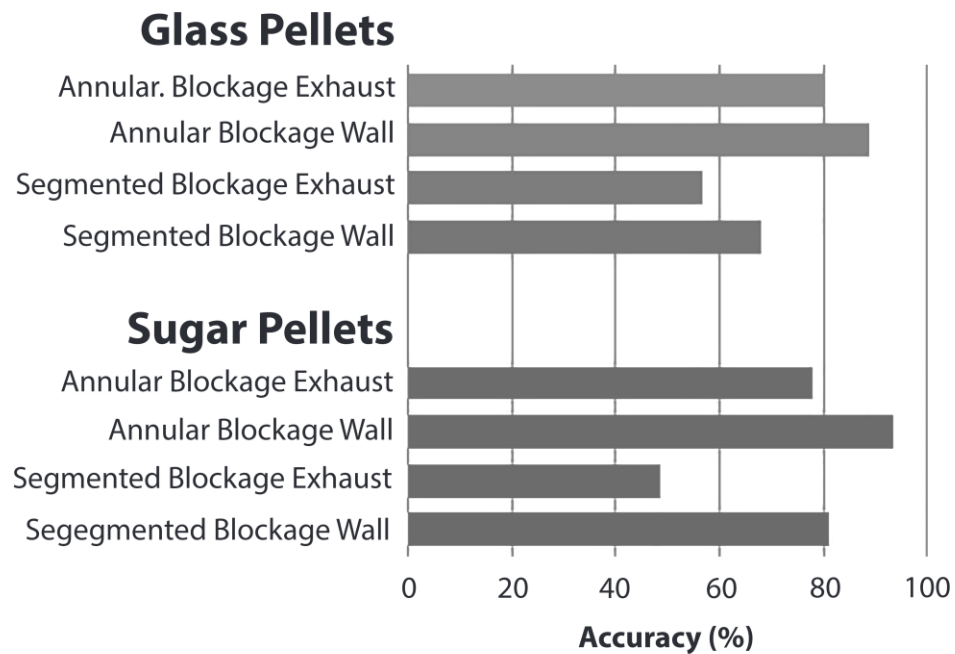

Figure 4.7 Deep learning evaluation using 10-fold cross validation accuracy for each material and blockage condition

Mean accuracy for the wall microphone was notably higher (82.7%) than mean accuracy for the exhaust microphone (65.8%). Accuracy for the glass pellets and sugar pellets were similar.

4.4   Discussion

The acoustic emissions from a fluidized bed process can be attributed to three sources: particle-particle collisions, particle-vessel collisions, and air flow through the bed and freeboard (18). Each of the three sources can be measured by either of the two microphones used during the experiments; however, air flow is believed to be the dominant source of passive acoustic emissions measured by the exhaust microphone while particle-wall collisions are believed to be the dominant source of passive acoustic emissions measured by the wall microphone. Figure 4.8 shows the observed fluidized bed behaviors focusing on the spouting or ejection of pellets into the freeboard.
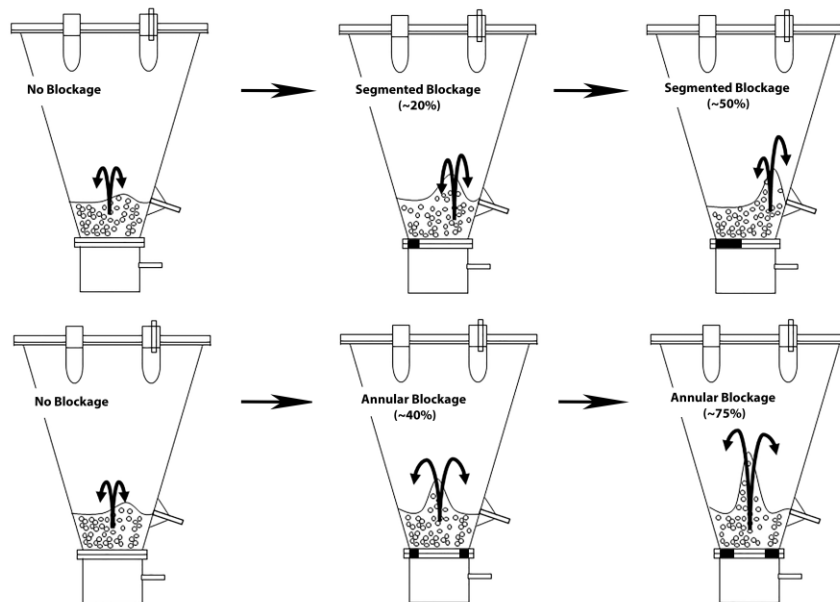

Figure 4.8 Visual observations of pellet spout as distributor plate blockage increased

Without blockage, the spout was centrally located and reached a height of about 0.2 m above the bed surface. The pellets from the spout fell back to the bed in a radial and

uniform pattern. As the annular blockage was introduced, the spout remained approximately centered in the bed. Defluidized zones that started from an outer annulus grew inward as the blockage increased. Due to the conical shape of the vessel combined with the circular flow pattern of the pellets, the effect of pellet velocities and their collisions with the vessel walls was complex. As the segmented blockage was introduced, the spout location shifted to the freely flowing space opposite to the blockage. With the radial change in spout location, a greater number of the ejected pellets collided with the vessel wall.

Higher velocities resulted in higher impact energies from the pellets spouting and falling against the sides of the chamber. This increase in impact energy subsequently affected the sound waves that were generated by each collision. As shown in Figures 4.5 and 4.6, the artificial neural network was able to use the passive acoustic emissions to reliably classify the blockage size using the wall microphone for annular and segmented blockage patterns.

The artificial neural network provided accurate blockage classification through the evaluation of 34 signal feature vectors that were extracted from each passive acoustic segment using pyAudioAnalysis. The network architecture contained multiple hidden layers of 22 nodes which assessed the relationships between feature and blockage classification, as well as the interdependent relationships between multiple features and blockage classification. This multivariate analysis was proven to be effective in predicting current blockage conditions inside the fluidized bed; however, in its current form is unable to indicate which of the 34 features is most important. A downside to

including hidden layers within the deep learning architecture is reduced transparency. The most dominate features or interdependent feature relationships remain unknown. A recent study evaluated the application of a parallel neural network to expose the hidden layers (19). Applying such methods to passive acoustic monitoring may be studied in future work. Selecting only dominant features for analysis would further reduce the computation requirements during in-line process control applications.

Figures 4.7 shows that the wall microphone was more effective for process control applications. The wall microphone provided 16.9% higher mean accuracy across all trials. The wall microphone is completely non-invasive when attached onto the exterior of the fluidized bed chamber. It has no interactions with materials inside the process boundary, making it ideal for pharmaceutical manufacturing environments. The exhaust microphone rests in a less ideal location as it can be exposed to process residual exiting the chamber. Depending on the application, the exhaust microphone may be impractical or require additional cleaning. The exhaust microphone recordings are expected to be more dependent on aerodynamic acoustic emissions developed from air passing through the chamber. Changes in the air flow path may alter the frequency and amplitude of sound waves that exit the exhaust.

As shown in Figures 4.5 to 4.7, the higher density glass pellets provided similar performance as the lower density Suglets®. It was originally hypothesized that the Suglets® would not perform as well as glass pellets because the lower density Suglets® release less energy upon impact. The data suggests that acoustic monitoring is robust and

can be applied to various cases in pharmaceutical, petrochemical, agriculture, or food processing industries.

Through completion of this research, it was determined that passive acoustic emissions can detect distributor plate blockages. As the magnitude of the distributor plate blockage increased, features within the sound waves changed. These small changes were effectively identified using an artificial neural network. Distributor plate blockage resulted in a higher range of pellet velocities. This shift in hydrodynamics subsequently resulted in a shift in passive acoustic emissions recorded by the microphones. The deep learning architecture successfully evaluated short-term time and frequency domain variations from a signal that could be used in real-time process control application.

4.5   Conclusions

The passive acoustic emissions monitoring combined with deep learning analytics proved to be effective for use in a process control application. In pharmaceutical manufacturing environments, a microphone placement outside the process boundary is ideal for operational control applications. Acoustic monitoring provides no risk of product contamination and can be a highly cost-effective solution to deter process failure. Passive sound waves created from industrious environments provide a wealth of untapped information. Deep learning in turn provides us with a new way to extract value from the sound. Without a doubt, the ease by which early artificial intelligence programs can decipher sound will play an active role in advancing industrial passive acoustic monitoring within the next decade.

4.6   References

1. Bauer W, Werther J, Emig G. Influence of gas distributor design on the performance of fluidized bed reactor. German Chemical Engineering. 1981;4:291–298.

2. Garncarek Z, Przybylski L, Botterill, J, Broadbent C. Quantitative assessment of the effect of distributor type on particle circulation. Powder Technology 1997;91:209–216

3. Wormsbecker M, Pugsley T. Distributor Induced Hydrodynamics in a Conical Fluidized Bed Dryer. Drying Technology. 2009;27(6):797-804.

4. Iveson S, Litster J, Hapgood K, Ennis B. Nucleation, growth and breakage phenomena in agitated wet granulation processes: a review. Powder Technology. 2001;117(1-2):3-39.

5. Sheahan T, Briens L. Passive acoustic emission monitoring of pellet coat thickness in a fluidized bed. Powder Technology. 2015;286:172-180.

6. Sheahan T, Briens L. Passive acoustic emissions monitoring of the coating of pellets in a fluidized bed—A feasibility analysis. Powder Technology. 2015;283:373-379.

7. W.R. Boyd J, Varley J. The uses of passive measurement of acoustic emissions from chemical engineering processes. Chemical Engineering Science. 2001;56(5):1749-1767.

8. Esteva A, Kuprel B, Novoa R, Ko J, Swetter S, Blau H et al. Dermatologist-level classification of skin cancer with deep neural networks. Nature. 2017;542(7639):115-118.

9. Golden J. Deep Learning Algorithms for Detection of Lymph Node Metastases From Breast Cancer. JAMA. 2017;318(22):2184.

10. Xiong H, Alipanahi B, Lee L, Bretschneider H, Merico D, Yuen R et al. The human splicing code reveals new insights into the genetic determinants of disease. Science. 2014;347(6218):1254806-1254806.

11. Geldart D. Types of gas fluidization. Powder Technology. 1973;7(5):285-292.

12. Ergun S, Orning A. Fluid Flow through Randomly Packed Columns and Fluidized Beds. Industrial & Engineering Chemistry. 1949;41(6):1179-1184.

13. Wen C, Yu Y. A generalized method for predicting the minimum fluidization velocity. AIChE Journal. 1966;12(3):610-612.

14. Giannakopoulos T. pyAudioAnalysis: An Open-Source Python Library for Audio Signal Analysis. PLOS ONE. 2015;10(12):e0144610.

15. Theano Development Team. Theano: A Python framework for fast computation of mathematical expressions. arXiv e-prints. 2015;arXiv:1603.04467

16. Abadi M, Agarwal A, Barham P, et al. TensorFlow: Large-Scale Machine Learning on Heterogeneous Distributed Systems. arXiv e-prints. 2016;arXiv:1603.04467

17. Chollet F, et al. Keras. GitHub repository. 2015; https://github.com/keras-team/keras

18. Tsujimoto H, Yokoyama T, Huang C, Sekiguchi I. Monitoring particle fluidization in a fluidized bed granulator with an acoustic emission sensor. Powder Technology. 2000;113(1-2):88-96.

19. Zeiler M, Fergus R. Visualizing and Understanding Convolutional Networks. arXiv e-prints. 2013;arXiv: 1311.2901

Chapter 5

Conclusions

New process analytical technologies will drive continuous improvement in the

pharmaceutical manufacturing space. PATs provide greater understanding of conditions

within the manufacturing environment and provide control over product quality. Under

the QbD framework, our ability to understand every aspect of the manufacturing process

reduces product safety risks and improves pharmaceutic outcomes. From an economic

view, new PATs will reduce operating cost by strengthening automation, and supporting

manufacturing optimization.

The objective of this work was to evaluate passive acoustic emissions monitoring as a

PAT for fluidized bed coating. Previous research has established that passive acoustic

emissions can be used to detect changes in a fluidized bed process; however further

research was required in understanding how process conditions, or unwanted process

events (such as distributor plate blockage) will affect the acoustic emissions.

Acoustic emissions are highly complex. The integration of deep learning for multivariate

data analysis in Chapter 4 applied a modern data workflow to extract meaning from the

data. The results not only demonstrated the performance of passive acoustic emissions

monitoring, but also demonstrated the effectiveness of deep learning for data analysis in

process control applications. The artificial neural network was able to study the

experimental data, learn patterns within the experimental data, and then accurately

predict process conditions based on independent data. Deep learning to enhance process control will reduce the risk of human error.

Passive acoustic emissions monitoring provides no risk of product contamination as the microphones are located outside the process boundary. The monitoring is non-destructive and highly cost-effective. Sound waves created from manufacturing environments provide a wealth of untapped information. At the same time, deep learning provides us a way to extract meaning from the sound.

Appendix A

Python Code used for Deep Learning Model

```python
# Deep Learning applied to Passive Acoustic Emissions after feature extraction from
PyAudioAnalysis

# Install Theano
# Install Tensorflow
# Install Keras

# Part 1 - Data Preprocessing

# Import libraries
import numpy as np
import matplotlib.pyplot as plt
import pandas as pd

# Import dataset
dataset = pd.read_csv('input_from_PyAudioAnalysis.csv')
X = dataset.iloc[:, 0:34].values
y = dataset.iloc[:, 34].values

# Split dataset into the Training set and Test set
from sklearn.model_selection import train_test_split
X_train, X_test, y_train, y_test = train_test_split(X, y, test_size = 0.2, random_state = 0)

# Feature Scaling
from sklearn.preprocessing import StandardScaler
sc = StandardScaler()
X_train = sc.fit_transform(X_train)
X_test = sc.transform(X_test)


# Part 2 - Build Deep Learning Model

# Import Keras library and packages
import keras
from keras.models import Sequential
from keras.layers import Dense

# Initialising the ANN
classifier = Sequential()

# Adding the input layer and the first hidden layer
classifier.add(Dense(units = 22, kernel_initializer = 'uniform', activation = 'relu', input_dim = 34))

# Adding the second hidden layer
classifier.add(Dense(units = 22, kernel_initializer = 'uniform', activation = 'relu'))
```

```
# Adding the output layer
classifier.add(Dense(units = 7, kernel_initializer = 'uniform', activation = 'softmax'))

# Compiling the ANN
classifier.compile(optimizer = 'adam', loss = 'sparse_categorical_crossentropy', metrics =
['accuracy'])

# Fitting the ANN to the Training set
classifier.fit(X_train, y_train, batch_size = 10, epochs = 100)


# Part 3 - Making predictions and evaluating the model

# Predicting the Test set results
y_pred = classifier.predict(X_test)
np.savetxt("y_pred.csv", y_pred, delimiter=",")

# Making the Confusion Matrix
from sklearn.metrics import confusion_matrix
y_pred_rev = pd.read_csv('y_pred_rev.csv')
cm = confusion_matrix(y_test, y_pred_rev)


# Part 4 – Evaluate model using k-fold cross validation

# Evaluating the ANN
from keras.wrappers.scikit_learn import KerasClassifier
from sklearn.model_selection import cross_val_score
from keras.models import Sequential
from keras.layers import Dense
from keras.layers import Dropout
def build_classifier():
    classifier = Sequential()
    classifier.add(Dense(units = 22, kernel_initializer = 'uniform', activation = 'relu', input_dim =
34))
    classifier.add(Dropout(0.1))
    classifier.add(Dense(units = 22, kernel_initializer = 'uniform', activation = 'relu'))
    classifier.add(Dropout(0.1))
    classifier.add(Dense(units = 7, kernel_initializer = 'uniform', activation = 'softmax'))
    classifier.compile(optimizer = 'adam', loss = 'sparse_categorical_crossentropy', metrics =
['accuracy'])
    return classifier
classifier = KerasClassifier(build_fn = build_classifier, batch_size = 10, epochs = 500,)
accuracies = cross_val_score(estimator = classifier, X = X_train, y = y_train, cv = 2)
mean = accuracies.mean()
variance = accuracies.std()
```

Curriculum Vitae

Post-secondary Education and Degrees:

Master of Engineering Science Biomedical Engineering Western University London, Ontario, Canada	2016-2018
Bachelor of Engineering and Applied Science Process Engineering Memorial University St. John's, Newfoundland, Canada	2008-2013

Related Work Experience

Graduate Research Assistant, Biomedical Engineering Western University, London, Ontario Canada	2016-2018
Teaching Assistant, Chemical and Biochemical Engineering Western University, London, Ontario Canada	2016-2018
Technical Contact Engineer Imperial Oil, Sarnia, Ontario Canada	2015-2016
Environmental Advisor Imperial Oil, Sarnia, Ontario Canada	2013-2015
Project Engineering Student Placement ExxonMobil, St. John's, Newfoundland Canada	2012-2012
Reservoir Engineering Student Placement ExxonMobil, St. John's, Newfoundland Canada	2012-2012
Project Engineering Student Placement ExxonMobil, St. John's, Newfoundland Canada	2011-2011
Process Engineering Student Placement Huskey Energy, St. John's, Newfoundland Canada	2010-2011
Site Engineering Student Placement B&J Catalano, Perth, WA Australia	2010-2010